NEXT GENERATION SMART BARREL SYSTEM FOR WORKZONE SAFETY ENHANCEMENT

FINAL REPORT ~ FHWA-OK-12-02

ODOT SP&R ITEM NUMBER 2232

Submitted to:

John Bowman, P.E.
Planning & Research Division Engineer
Oklahoma Department of Transportation
200 N.E. 21st Street
Oklahoma City, Oklahoma 73105

Submitted by:

Yan Zhang, PhD, Principal Investigator
Hernan Suarez, PhD Student
Sudantha Perera, PhD Student
Radar Innovations Laboratory
School of Electrical and Computer Engineering
150 Devon Energy Hall
University of Oklahoma
Norman, Oklahoma 73019-1102



March 2012

TECHNICAL REPORT DOCUMENTATION PAGE

1. REPORT NO.	2. GOVERNMENT ACCESSION NO.	3. RECIPIENTS CATALOG NO.
FHWA-OK-12-02		

4. TITLE AND SUBTITLE	5. REPORT DATE
Next Generation Smart Barrel System for Workzone Safety Enhancement	**Jan 2012**
	6. PERFORMING ORGANIZATION CODE
7. AUTHOR(S)	8. PERFORMING ORGANIZATION REPORT
Yan (Rockee) Zhang, Hernan Suarez and Sudantha Perera	
9. PERFORMING ORGANIZATION NAME AND ADDRESS	10. WORK UNIT NO.
University of Oklahoma, School of Electrical and Computer Engineering Devon Energy Hall, Room 150, Norman, Oklahoma 73019-6141	11. CONTRACT OR GRANT NO. **ODOT SP&R Item Number 2232**
12. SPONSORING AGENCY NAME AND ADDRESS	13. TYPE OF REPORT AND PERIOD COVERED
Oklahoma Department of Transportation 200 N.E. 21st Street, Room 3A7, Oklahoma City, OK 73105	Final Report **October 2010 to Dec 2011**
	14. SPONSORING AGENCY CODE

15. SUPPLEMENTARY NOTES

16. ABSTRACT

The Radar Innovations Lab in the University of Oklahoma collaborated with the P&R Division of OK-DOT on an innovative technology for traffic speed monitoring and control in high-way workzones, called Smart Barrel Systems. The smart barrel system appears as a group of normal traffic control barrels, but they are equipped with advanced and low-cost Doppler radar sensor and wireless radio nodes. The traffic speeds are monitored by a sensor node at the workzone entrance in real-time, and then all the nodes in the network coordinate among each other to determine the warning message to motorists, which in this case is the flashing LED lights on top of the barrel drums. There are six tasks in this one-year project: (1) Requirement analysis and specifications, (2) Simulation/Modeling, (3) Design and test a Doppler radar sensor, (4) ZigBee radio testbed platforms, (5) Prototype smart barrels, (6) Meetings and reports.

As an extension of the originally planned task 5, a small-scale (10-node) smart barrel system is integrated and deployed at an actual workzone site at I-40, during the period of Aug- Dec 2011. Significant speed reduction has been observed by comparing the traffic speed profile entering the "smart workzone" to the speed profile leaving the zone. A series of improvements have been made for better synchronization of the nodes/lights, longer battery life, and lower costs.

17. KEY WORDS	18. DISTRIBUTION STATEMENT
Workzone safety, radar, traffic speed, speed monitoring and control	**No restrictions. This publication is available from the Planning & Research Div., Oklahoma DOT.**

19. SECURITY CLASSIF. (OF THIS REPORT)	20. SECURITY CLASSIF. (OF THIS PAGE)	21. NO. OF PAGES	22. PRICE
Unclassified	**Unclassified**	**58**	**N/A**

Disclaimer

The contents of this report reflect the views of the author(s) who is responsible for the facts and the accuracy of the data presented herein. The contents do not necessarily reflect the views of the Oklahoma Department of Transportation or the Federal Highway Administration. This report does not constitute a standard, specification, or regulation. While trade names may be used in this report, it is not intended as an endorsement of any machine, contractor, process, or product.

SI* (MODERN METRIC) CONVERSION FACTORS

APPROXIMATE CONVERSIONS TO SI UNITS				
SYMBOL	WHEN YOU KNOW	MULTIPLY BY	TO FIND	SYMBOL
LENGTH				
in	inches	25.4	millimeters	mm
ft	feet	0.305	meters	m
yd	yards	0.914	meters	m
mi	miles	1.61	kilometers	Km
AREA				
in^2	square inches	645.2	square millimeters	mm^2
ft^2	square feet	0.093	square meters	m^2
yd^2	square yard	0.836	square meters	m^2
ac	acres	0.405	hectares	Ha
mi^2	square miles	2.59	square kilometers	km^2
VOLUME				
floz	fluid ounces	29.57	milliliters	mL
gal	gallons	3.785	liters	L
ft^3	cubic feet	0.028	cubic meters	m^3
yd^3	cubic yards	0.765	cubic meters	m^3
NOTE: volumes greater than 1000 L shall be shown in m^3				
MASS				
oz	ounces	28.35	grams	G
lb	pounds	0.454	kilograms	Kg
T	short tons (2000 lb)	0.907	megagrams (or "metric ton")	Mg (or "t")
TEMPERATURE (exact degrees)				
^oF	Fahrenheit	5 (F-32)/9 or (F-32)/1.8	Celsius	^oC
ILLUMINATION				
fc	foot-candles	10.76	lux	Lx
fl	foot-Lamberts	3.426	$candela/m^2$	cd/m^2
FORCE and PRESSURE or STRESS				
lbf	poundforce	4.45	newtons	N
lbf/in^2	Poundforce per square inch	6.89	kilopascals	kPa
APPROXIMATE CONVERSIONS FROM SI UNITS				

SYMBOL	WHEN YOU KNOW	MULTIPLY BY	TO FIND	SYMBOL
LENGTH				
mm	millimeters	0.039	inches	in
m	meters	3.28	feet	ft
m	meters	1.09	yards	yd
km	kilometers	0.621	miles	mi
AREA				
mm^2	square millimeters	0.0016	square inches	in^2
m^2	square meters	10.764	square feet	ft^2
m^2	square meters	1.195	square yards	yd^2
ha	hectares	2.47	acres	ac
km^2	square kilometers	0.386	square miles	mi^2
VOLUME				
mL	milliliters	0.034	fluid ounces	floz
L	liters	0.264	gallons	gal
m^3	cubic meters	35.314	cubic feet	ft^3
m^3	cubic meters	1.307	cubic yards	yd^3
MASS				
g	grams	0.035	ounces	oz
kg	kilograms	2.202	pounds	lb
Mg (or "t")	megagrams (or "metric ton")	1.103	short tons (2000 lb)	T
TEMPERATURE (exact degrees)				
^oC	Celsius	1.8C+32	Fahrenheit	^oF
ILLUMINATION				
lx	lux	0.0929	foot-candles	fc
cd/m^2	$candela/m^2$	0.2919	foot-Lamberts	fl
FORCE and PRESSURE or STRESS				
N	newtons	0.225	poundforce	lbf
kPa	kilopascals	0.145	poundforce per square inch	lbf/in^2

*SI is the symbol for the International System of Units. Appropriate rounding should be made to comply with Section 4 of ASTM E380.

Table of Contents

SI* (MODERN METRIC) CONVERSION FACTORS iv
EXECUTIVE SUMMARY xii
1. INTRODUCTION 1
2. Summary of Requirement Analysis 2
2.1 The deployment of the smart barrel system 2
2.2 The test and evaluations of the system 3
3. Simulation Evaluation of Smart Barrel Systems 3
3.1 Basic Simulation Configurations 3
3.2 ZigBee Network Behavior Simulation Results 5
3.3 Power Consumption and Battery Life Evaluations 7
4. The ZigBee and Wireless Network Platform 9
4.1 ZigBee Product Selection 9
4.2 Wireless Communication Link Test 12
4.3 ZigBee Transceiver Integration 14
4.4 Data Logger Incorporation 17
5. The Radar Sensor Developments 18
5.1 X-band, Low Cost Doppler Radar Sensor 18
5.2 K-band, High Quality Doppler Radar Sensor 23
6. System Integration and Initial Field Deployments 26
6.1 Overview of the Prototype Smart Barrel System 26
6.2 Network Configurations 28
6.3 Software Implementations 30
6.4 Node Integrations 31
6.5 Field Deployment Arrangements 43
6.6 Speed Monitoring Data Records and Analysis Results 44
6.6.1 Field tests and data collection on Aug 28, 2011 44
6.6.2 Discussion of the initial deployment data results until end Sep 2011 47
6.6.3 Oct 2011 data record and analysis 49
6.6.4 Data Records and Analysis of November 2011 52

7. Conclusions and Recommendations 57
REFERENCES 58

List of Figures

Figure 1: ZigBee elements and Mesh/Star topology. 4
Figure 2: End to End Delay. 4
Figure 3: Mesh topology in OPNET simulator. 4
Figure 4: Sensor parameters using OPNET-ZB model. 5
Figure 5: Battery-energy consumption of network. 5
Figure 6: Network output load. 6
Figure 7: Battery remaining for the second endpoint. 6
Figure 8: Radio receiver bit error rate. 6
Figure 9: Network battery power consumption. 7
Figure 10: Network throughput Load. 7
Figure 11: Battery life estimation for different average speeds. 8
Figure 12: Battery life estimation for different values of average day traffic density. 8
Figure 13: Xbee development boards 9
Figure 14: X-CTU software tool. 9
Figure 15: Arduino Uno development platform. 10
Figure 16: Data collected from the analog input. 10
Figure 17: XBee module mounted on the Arduino Uno board. 11
Figure 18: Base module over a block of concrete. 12
Figure 19: Mobile node connected to a laptop. 12
Figure 20: Percentage of packets received for different distances. 13
Figure 21: Signal Strength of the last packet. 13
Figure 22: A more complete ZigBee test unit platform was assembled with the Doppler sensor on the top, and the microcontroller (MCU) board at the bottom. 14
Figure 23: Serial link between the microcontroller and the Xbee module. 14
Figure 24: Wireless network diagram with ZigBee nodes 15
Figure 25: Wireless network configuration during lab test stage: source device, router, and remote device. 15
Figure 26: Testing of the network communication topologies. 16
Figure 27: Data logger shielded with a SD card. 17
Figure 28: Data logger integrated into the transceiver module. 17
Figure 29: Lab test of the basic functions of a low-cost X-band prototype Doppler radar sensor. 18
Figure 30: Doppler Radar Intermediate Frequency (IF) stage schematic circuit 19
Figure 31: PCB layout 19
Figure 32: Doppler radar moving target signature recorded by the microcontroller. 20
Figure 33: Developed real-time PC interface showing Doppler radar signal. 20
Figure 34: Initial outdoor test of Doppler radar sensor. 21
Figure 35: Initial setup of the radar sensor tests. 21
Figure 36: Collecting data on High Way 9. 22
Figure 37: Sample recorded traffic data with low-sensitivity mode. 22

Figure 38: Sample recorded traffic flow data with high-sensitivity mode. 23
Figure 39: Initial setup of the *higher power* radar sensor node. 24
Figure 40: Statistical traffic data collection setup on High-Way 9. 24
Figure 41: A LabVIEW interface showing recorded speed of vehicles. 25
Figure 42: A snapshot of the statistical traffic speed data on HWY#9, based on higher power radar sensing node. The estimated radar data rate is 5-6 samples/sec. 25
Figure 43: Measured speed data for individual vehicle tend to decrease with time as the vehicle leaves the radar beam, and the vehicles in adjacent lanes may have effects too. 26
Figure 44: Smart barrel node internal architecture. The higher power (radar) node containing K-band radar sensor. 27
Figure 45: Smart barrel node internal architecture .The lower-power (radio) node with data logger. Data logger is not necessary for all the radio nodes. 27
Figure 46: Warning lights in dim mode at night when no speeding is detected. 28
Figure 47: Warning lights flashing when speeding is detected. 28
Figure 48: ZigBee Network configuration #1 29
Figure 49: ZigBee Network configuration #2. 29
Figure 50: General Flow chart for data handling and LEDs control in each node. 31
Figure 51: Initial system integration on a sample barrel: it includes the X band low-power sensor, Arduino Uno microcontroller, XBee module, and RGB LEDs. 32
Figure 52: Testing a CMOS voltage level shifter circuit. 33
Figure 53: RS232 to TLL voltage level converter circuit. 33
Figure 54: The RGB matrix of LEDs shows speed in green because the moving objective lowers than the pre-configured speed limit of 10 mph. 34
Figure 55: The RGB matrix of LEDs shows speed in red because the moving objective exceeds the pre-configured speed limit of 10 mph. 34
Figure 56: Mechanical housing for the high-power node. 35
Figure 57: Mechanical housing for the low-power node. 35
Figure 58: Mounting of the three laboratory prototype nodes. 36
Figure 59: System configuration with four nodes. 36
Figure 60: View of the zone. 37
Figure 61: Higher power node 37
Figure 62: LabVIEW interface registering speed data. 37
Figure 63: Type-A blue warning light 38
Figure 64: Type-B amber warning light. 39
Figure 65: Interfacing radar sensor, microntroller, XBee radio, and LEDs. 39
Figure 66: Low-power node integrated with a solar panel and a rechargeable battery. 40
Figure 67: High-power node integration. 40
Figure 68: PCB board includes a MCU and an XBee radio. 41
Figure 69: Data logger shield with a SD card holder which has a 16GB microSD card. 41
Figure 70: The 10 programmable modules labeled with their respective address. 42
Figure 71: The 10 warning lights ready to be mounted on the traffic barrels. 42

Figure 72: Deployment zone location: 35°28'00.41" N 97°43'19.79" W. Warning message board: “flashing light ahead if speeding”. 43
Figure 73: Deployment of the nodes along the construction site. 44
Figure 74: Team deploying the warning lights during daylight 45
Figure 75: High power node was still working after three days of the installation. 45
Figure 76: Plot of the first 100 minutes of continuous data. Mean speed= 61.153mph, and STD= 4.816mph. 46
Figure 77: Plot of the first 100 minutes of continuous data. Mean speed= 60.42mph, and STD= 3.44mph. 47
Figure 78: Plot of 16.6 hours of continuous data. Mean speed= 61.69mph, and STD= 3.92mph. 47
Figure 79: 8 hour traffic Aug 28, low-flashing Rate, entrance of zone 48
Figure 80: 8 hour traffic Sep 26, high-flashing Rate, entrance of zone 48
Figure 81: 7.5 hour traffic Sep 19, high-flashing Rate, exit of zone. 49
Figure 82: Oct 6 data – Radar 1: 12 AM -9AM. 50
Figure 83: Oct 6 data- Radar 2: 12 AM-9AM. 50
Figure 84: Radar 1: 7PM-12AM. 51
Figure 85: Radar 2: 7PM-12AM. 51
Figure 86: Comparison of the average traffic speed collected by the two K-band radar sensors on 10-05-11 with histograms. 52
Figure 87: Comparison of the average traffic speed collected by the two K-band radar sensors on 10-06-11 with histograms. 52
Figure 88: Warning lights in dim mode at night when no speeding is detected. 53
Figure 89: Warning lights flashing when speeding is detected. 53
Figure 90: Comparison of the average traffic speed collected by the two K-band radar sensors on 10-30-11. Radar sensor 1 was set up at 15:28, and Radar sensor 2 at 16:28. 54
Figure 91: Comparison of the average traffic speed collected by the two K-band radar sensors on 10-31-11. 55
Figure 92: Comparison of the average traffic speed collected by the two K-band radar sensors on 11-01-11. 55
Figure 93: Comparison of the average traffic speed collected by the two K-band radar sensors on 11-02-11. 56
Figure 94: Comparison of the average traffic speed collected by the two K-band radar sensors on 11-03-11. 56

List of Tables

Table 1: Parameters for battery life estimation 7
Table 2: K-band Doppler Radar Sensor Specifications 23
Table 3: Nov 2011 field test general information 54

EXECUTIVE SUMMARY

This one-year research project is supported by ODOT Planning and Research Division, the performance period (FY11) is Oct 2010 to Dec 2011. The Radar Innovations Lab (currently Radar Innovations Center) in the University of Oklahoma has been the technical working team.

The objectives of this research project:

To verify the smart barrel system implementation can provide speed alert/warning and reduce collision risk.
To demonstrate that a future smart barrel product and the cost, battery life and deployments.
Design and test a very low-cost, low power Doppler radar sensor to meet specifications.
Demonstrate the accuracy, efficiency and reliability of mobile computing paradigm in workzone collision warning application.

Project Deliverables:

Final research report.
Three project meetings with ODOT.
The prototype smart barrel system including radar sensor nodes and radio nodes.
Field tests results.
2 to 4 page color article.
Monthly progress reports – Submitted as required.

Scope of Work:

Task 1: Specify system requirements
Task 2: Simulation tools to predict the system performance and deployment costs
Task 3: Design and test a Doppler radar sensor
Task 4: Acquire the latest ZigBee development and control kit and develop ZigBee-based distributed control software
Task 5: Integrate and field test smart barrel modules together with preliminary site supervisor software
Task 6: Meetings, reports and deliverables.

Methodology:

This project is an application of intelligent sensor network to transportation systems. A product-development approach has been taken from the beginning. As a “standard” wireless sensor node, industrial standard (ZigBee) wireless protocols and transceivers are used. To save cost and development time for prototyping, OEM sensor package is used and integration of sensor nodes is based on modifying the existing type B traffic barrel LED lights. At the software side, we investigated different possible network configurations, and have used the simplest configuration and mobile computing scheme in the field deployments. In the future development and production, a fully customized design and integration is possible, and more power-efficient network configuration scheme can be utilized.

Conclusions:

The technical feasibility of the smart barrel system has been well-demonstrated. The field deployment of the prototype system has validated the effectiveness of the smart barrel system as a traffic monitoring and alert tool. In order to achieve a matured new product, we must further address these following challenges: (1) Batteries, using commercial lantern batteries, the prototype has already had battery life comparable, or even longer than the current barrel lights on the market. However, the current enclosure does not accommodate the size of the batteries, and we still need to manually change the batteries. (2) Costs. The radar sensor is working very well, and it can become a little bit pricy if we need more radar sensor nodes in a network. (3) The further evaluation of the impact of this system to actual road environment. This include better packaging of the devices for environment resistant, more importantly, human factor impacts need to be further evaluated to analyze the responses from motorists.

1. INTRODUCTION

According to Federal Highway Administration's safety program, the nation has about one workzone related fatality every 10 hours (2.3 a day), or one work zone injury every 13 minutes (110 a day). The goal of the proposed project is reducing workzone–related crashes, accidents and congestions through an intelligent sensing and warning system based on IEEE 802.15.4 (ZigBee) network protocol and microwave Doppler sensor.

The concept of "smart barrel" system can be traced back to 2005 when the University of Michigan completed a project for FHWA (Sullivan J et.al 2005). In their reports, they suggested the solution of using multiple sensors for traffic speed monitoring, and using wireless LAN networks for inter-node communications. There has been interesting work done in that project about selecting and comparing multiple sensors (camera, optical, ultrasound, and magnetic sensors), as well as some initial investigation on human factors and warning message designs. However, it was found that the wireless LAN protocol and the centralized "site supervisor" architecture can become a severe bottleneck for the reliability and scalability of the system.

In the commercial market, there are some vendors have claimed various levels of intelligence in the traffic barrel products. The "i-Cone" product (i-Cone Products Website 2011), for example, uses global positioning system (GPS) inside a barrel drum for self-localization, and communicates through the web for traffic information. There is no warning or control messaging functions in this product, the communication/localization technologies are expensive and usually only used in trailer-based speed monitoring and messaging system (according to Action Safety, a single trailer based speed monitoring and messaging unit can cost $18K-$20K).

In terms of warning message, the LED lights are the dominant mechanism for traffic barrels. Most of the construction projects use the so called "Type-A" lights, which have lower brightness, only operate during the nights, and do not flash. In some more important zones or complex construction sites, the brighter "Type-B" light is used, which operates both day and night, and flashes at some fixed rates. There is no coordination among the lights in different drums.

Manufactures have come up with barrel lights with better synchronization among each other. The so called *sequential light* is one of the latest products. A good example is the synchronized sequential lights from C&C Signal, called Synchro-Solar and Synchro-D barricade lights, which are able to flash sequentially for road guidance. It is not sure how the sequential timing control is done for this product, but the technique of using optical or laser alignment among the adjacent nodes have been reported. Again, there is no traffic speed monitoring function for such products and the mechanism for synchronization is not very reliable.

The smart barrel system proposed in this project can potentially fill the gap between the traffic monitoring and speed messaging in a new low-cost, integrated, scalable and reliable configuration. First, the traffic monitoring and messaging are done in real-time and locally, there is no need for central or remote control centers. The "collaboration" among the node can be

highly intelligent, in the way that they can communicate each other as a mesh network. Each barrel node, as a so-called “software agent”, receives traffic information from other nodes in the zone and decide how to generate warning signals. The highly integrated Doppler radar sensor and standard ZigBee-type radar transceivers are used in the smart barrel nodes. In short, the smart barrel system in this project is a distributed sensing and control system with networked nodes.

The potential benefits of the proposed technology include automatic multiple functions (traffic monitoring and control), lower cost, good scalability, and system reliability (if some of the nodes are knocked down or damaged, the system can “self-heal” by node re-organizing). Functionality wise, it provides a real-time speed alert to both motorists and the workers in the zone. It generates such warnings in high spatial and time resolution, and very specific for dedicated areas. Therefore, it is complementary to the trailer based speed messaging system for overall safety enhancement.

The time and budget of this project allows us to promote this system technology from multiple aspects and in small scales. First, we did analysis of the application requirements of smart barrel systems. Second, we performed modeling and simulations of different network configurations, and performance evaluation for simulated large-scale system deployments. In the third task, we generated our own Doppler radar design and at the same time, we integrated and calibrated the commercial OEM radar sensors for field development unit prototypes. In the fourth task, we acquired, tested, and programmed ZigBee transceiver units from Digi-International. Finally, in technical Task5, we did actual field deployment of a small scale (10 nodes) smart barrel system and collected traffic monitoring data on a site at I-40.

2. Summary of Requirement Analysis

During the initial period of the project and kickoff meeting (Oct 11, 2010), the team has discussed with ODOT on the basic requirements of a smart barrel system.

2.1 The deployment of the smart barrel system

(1) The warning mechanism needs to be carefully selected and conform to state laws.

An immediate question is what kind/color/frequency of LED flashing lights we may choose. Initial discussions result in the consideration of a combination of Red and Amber flashing LED lights. The detailed implementation policies of warning signals can be elaborated in the future as they can be easily re-programmed according to the needs and site-specific parameters.

(2) The need of having an early detection of warning, with text messages to tell the meaning of the warning in the workzone, and initial speed alerts.

This is recognized as a very important issue as the drivers need initial alerts on speeds and know the meaning of flashing lights. The text-message can be placed on a front-end trailer before entering the workzone for this purpose. Also as the network coordinator, this trailer

collect the real-time traffic information within the workzone and gives an early notice to the driver what to expect ahead. Also, it gives warning to the crews in the workzone, through a siren type of sound in the workzone, via the wireless link if it detects a fast offender approaching.

(3) What kind of workzones the system is expected to deploy.

Shoulder-work zones may be application examples. It is important to consider this system to combine together other existing traffic control tools, such as concrete dividers and speed radar trailers.

2.2 The test and evaluations of the system

(1) Need to see if this system can effectively slow-down the traffic, reduce collision and enhance the safety. This will involve field tests and add feedback for the system design revisions. In terms of test site selection, naturally we need to start from a parking lot, driveways and local streets. A good local test site is Hwy 9 in Norman. The initial tests will only involve a small-scale network (with 4-5 full functional nodes) and as many as dummy drums. We may try to use another ZigBee radio vendor for larger network. The main purpose of this year of project is to validate the technical feasibility of the system concepts.

(2) Need to avoid 'over-alert' which cause the driver suddenly reduce speed and add potential of rear collision. This has to be achieved by carefully programming the strength and intensity of flashing warning and usage of early warning at front end.

3. Simulation Evaluation of Smart Barrel Systems

3.1 Basic Simulation Configurations

Simulation is an important task for verifying some basic concepts of the proposed distributed computing scheme. In the most of the stages, we have been using the software tool called OPNET. Different ZigBee architectures and functioning nodes, including coordinators, routers and end pointswere setup in the OPENT environment, the configuration shown in Figures 1-2 are able to predict end-to-end message latencies, which is important to syncronize the elements of the entire smart barrel system given the scale of the network (from the first node in the row to the last one in the end). It was then necessary to extend the simulator's libraries to be able to predict the power consumption and realistic data traffic models, with the aided of open-source version of OPEN-ZB: http://www.open-zb.net/wpan_simulator.php.

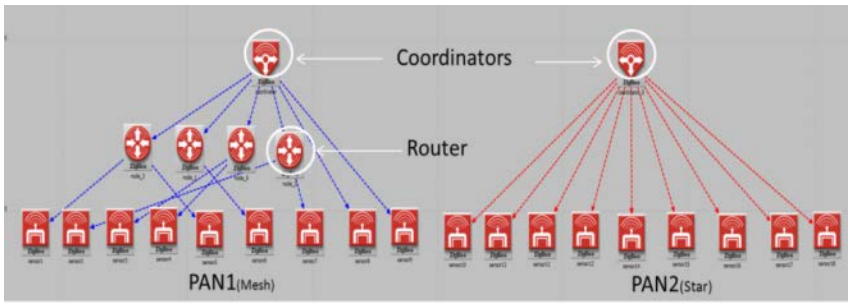

Figure 1: ZigBee elements and Mesh/Star topology.

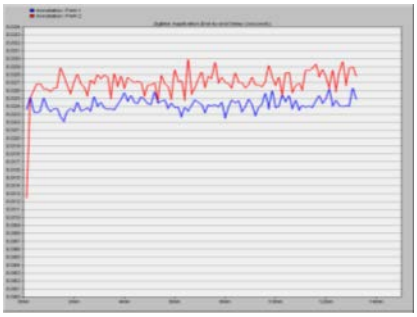

Figure 2: End to End Delay.

The open-source OPNET-ZB model was successfully incorporated to our OPNET environment, and different topologies were analyzed along with the communication tradeoffs. Some topologies and acquired and performance data from simulation are shown in Figure 3 and Figure 4 as screen displays.

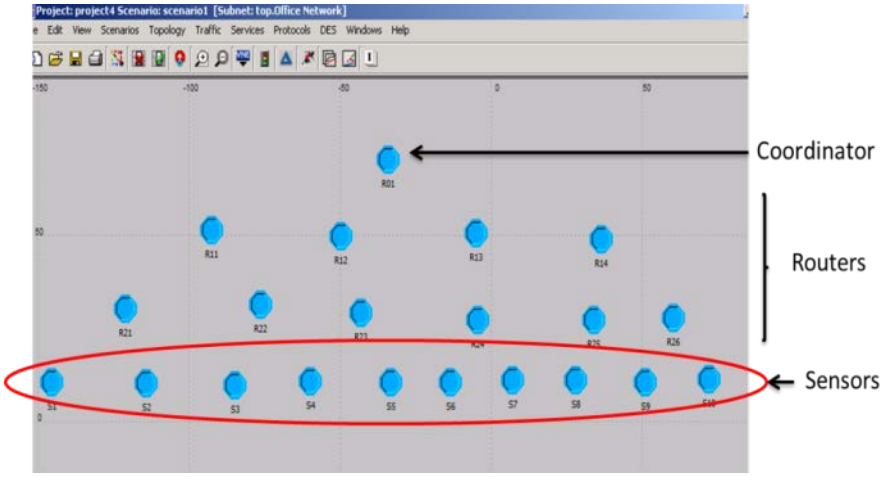

Figure 3: Mesh topology in OPNET simulator.

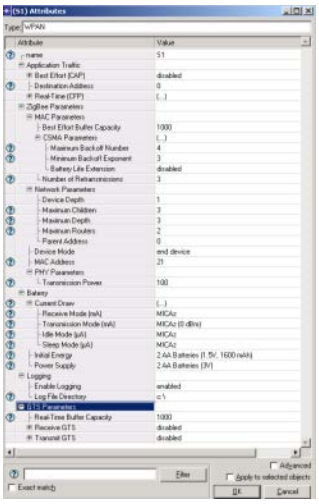

Figure 4: Sensor parameters using OPNET-ZB model.

3.2 ZigBee Network Behavior Simulation Results

A complete simulation based on OPNET was performed for a ZigBee network consisting of four endpoints and a coordinator. For this case, constant traffic was generated in each endpoint with the following parameters: Application traffic: Best effort (CAP); Packet interval time: 0.3 sec; Packet size: constant 100 bits; Simulation time: 10 minutes. Figure 5 and 6 show battery consumed energy and network output load (throughput).. For this four node system, we can see the average traffic load is about 1Kbit/sec, the periodic peak energy consumption less than 0.02 J, and the static energy consumption about 1/10 of the peaks.

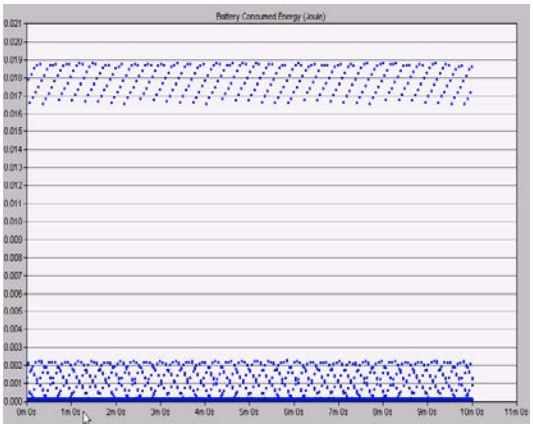

Figure 5: Battery-energy consumption of network.

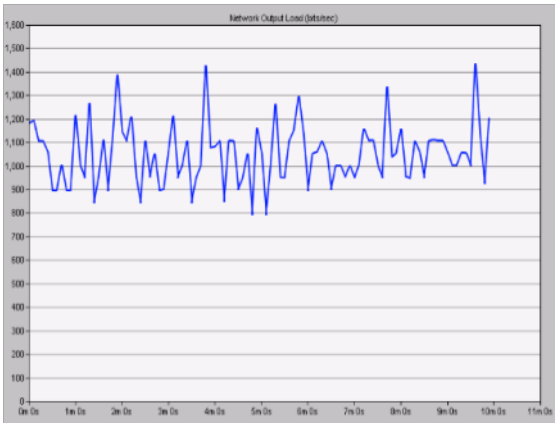

Figure 6: Network output load.

Also, for a single node in the network, we observe in Figure 7 that the battery remaining of the second node decreases linearly respect to the time, and the energy consumed in 10 min by the second node is very low, this estimation is without considering the power consumption from other elements of the system. The result of this small network will be scaled up to larger networks and will be made more realistic to the specific traffic our smart barrel system generates.

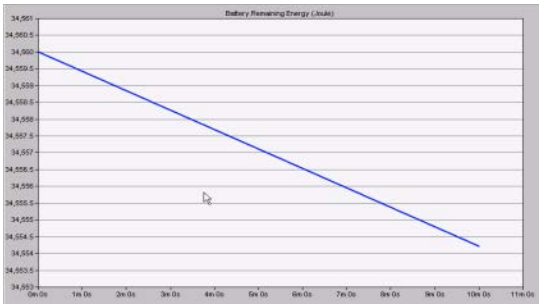

Figure 7: Battery remaining for the second endpoint.

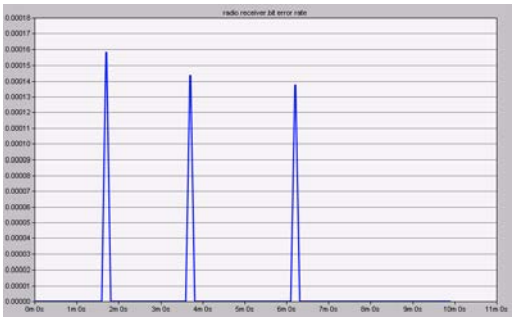

Figure 8: Radio receiver bit error rate.

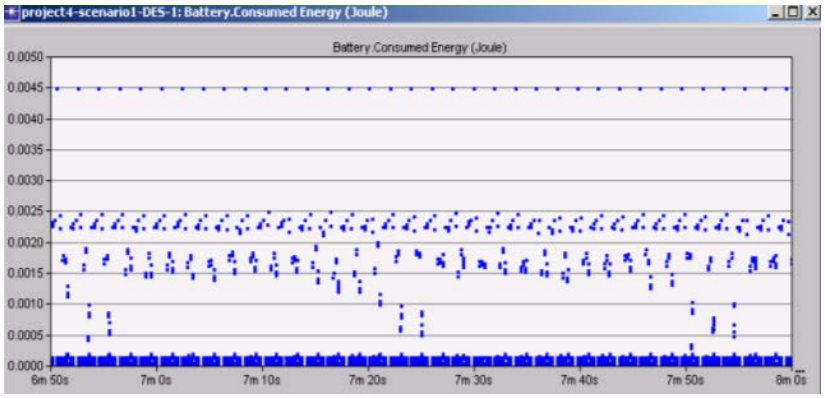

Figure 9: Network battery power consumption.

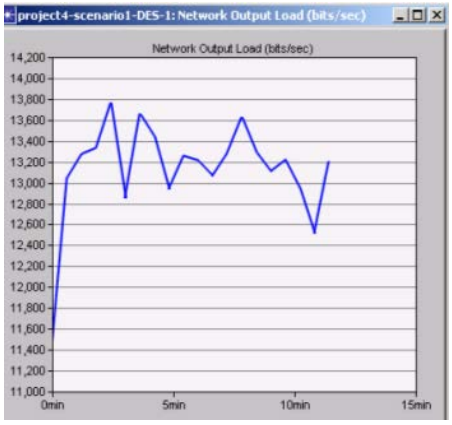

Figure 10: Network throughput Load.

3.3 Power Consumption and Battery Life Evaluations

Further battery life calculations for the sensor-ZigBee nodes integrated with a *higher power* K-band Doppler radar, including a display (1W), were approximately evaluated considering the following parameters:

Table 1: Parameters for battery life estimation

	Simulation 1	Simulation 2
Avg. day time traffic density (vehicles/hour)	400	X
Avg. night time traffic density (vehicles/hour)	20	30
Avg. Speed	X	40
Battery Voltage(V)	12	12
Battery Capacity(Amp*Hour)	40	40
Display Max Power(W)	1	1
K-band Radar Power(W)	0.11	0.11

Simulation results show that the higher average speed, the longer battery life, the main reason is because the vehicle will need less time to cross the radar beam so that the radar will use less energy to tack the speed of the vehicle. By establishing appropriate time frames in each detection period, a good balance between expected average traffic speed and power consumption can be achieved. Another important parameter is the average traffic density because it affects the battery life as it is shown in Figure 12.

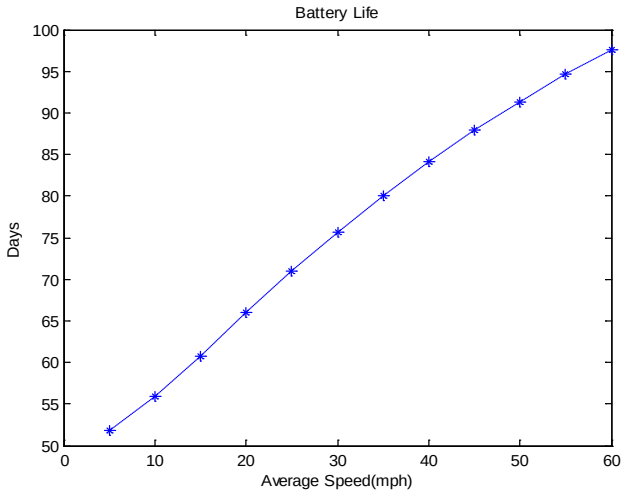

Figure 11: Battery life estimation for different average speeds.

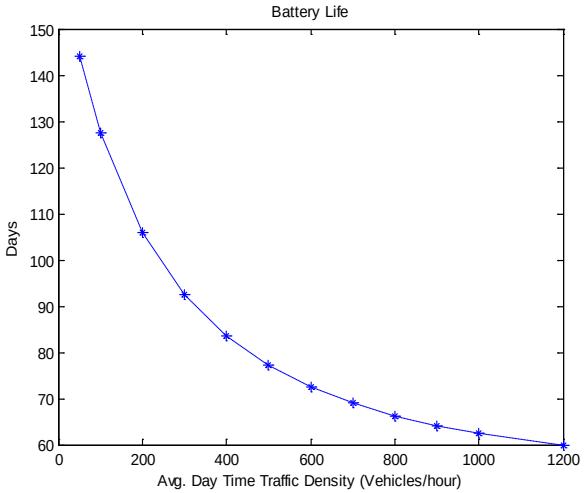

Figure 12: Battery life estimation for different values of average day traffic density.

We have evaluated the performance of 6 V batteries in simulation with two nodes and blinking the LEDs with different flashing rates for at least 3 days. In terms of battery life, the simulation results so far have been in accordance with field observations. The simulation of the radio-communication in the network has allowed testing on different configurations not available for the field tests at this point.

4. The ZigBee and Wireless Network Platform

4.1 ZigBee Product Selection

From the beginning of the development, the DigiMesh modules are adopted, they provide identical protocol sets as the ZigBee and lower cost. DigiMesh is developed by Digi International and presents some interesting features than ordinary ZigBee devices such as more flexibility to expand the network, programable option to sleep all nodes, peer to peer network, fully mesh capabilities, and multi-function nodes.

The Xbee DigiMesh development boards were configured and tested using the X-CTU software tool provided by Digi International. In Figure 13, the Xbee Pro DigiMesh development board is connected to a computer, and the Xbee DigiMesh development board to a null modem, computer sends a string of characters “Tx-PC” through the Xbee Pro module to the other module, and then the null modem sends the string back to the computer. Figure 14 shows the string of characters received on computer.

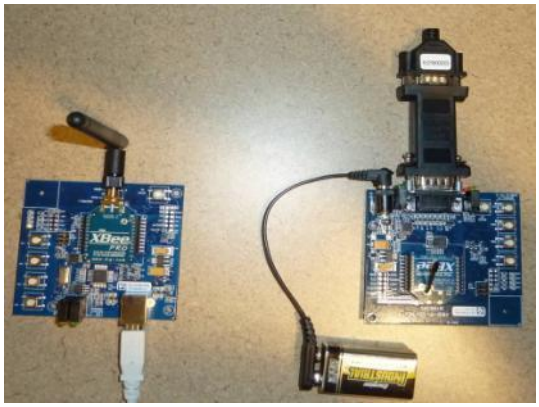

Figure 13: Xbee development boards

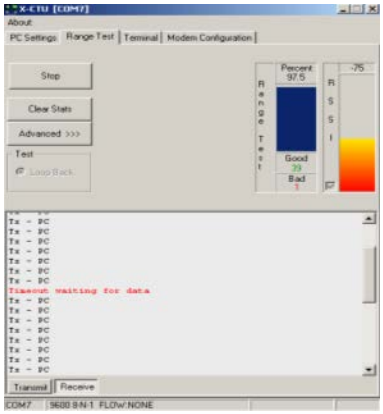

Figure 14: X-CTU software tool.

The Arduino Uno platform, which includes an ATMega328 microntroller from Atmel, was chosen to process and estimate the speed of a vehicle based on the Doppler radar sensor measurement. Using the Arduino IDE, the platform was programmed to turn on and off LEDs repeatedly. Also, the RS-232 serial connection between the board and a PC was tested successfully (as shown in Figures 15 and 16).



Figure 15: Arduino Uno development platform.

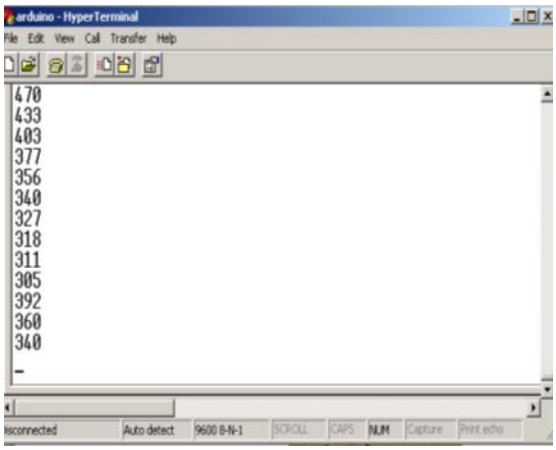

Figure 16: Data collected from the analog input.

As the next step toward a fully embedded module, a ‘shield’ with the Xbee DigiMesh chip was mounted on top of the microcontroller board to communicate with the wireless module through the serial ports. A framework of program (in C) were written for intelligent networking functions.

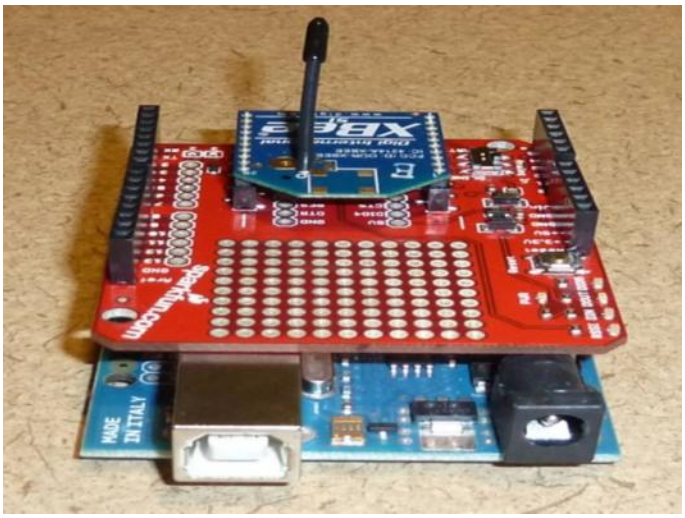

Figure 17: XBee module mounted on the Arduino Uno board.

4.2 Wireless Communication Link Test

The effective communication range of the Xbee/Digimesh modules was tested outdoor at the OU-Loyd Noble Center parking ground on Nov 20th 2010. The photos of experiment setup are shown in Figure 18 and 19 and recorded communication quality data is plotted in Figure 20 and 21. The ZigBee transmitter and receivers were placed at a height similar to a typical traffic barrel, and during the test the distance between the base and the remote module was increased while the percentage of packets received and signal strength were monitored on a laptop. It is observed that a **40**-**50 meters** reliable communication range can be expected for this ZigBee unit, depending on antenna type and orientations. This was an important parameter to determine the final topologies of the smart barrel networks.

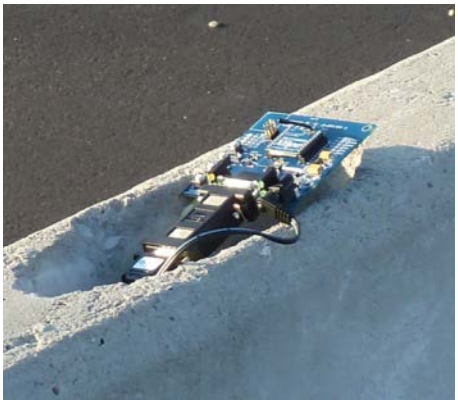

Figure 18: Base module over a block of concrete.



Figure 19: Mobile node connected to a laptop.

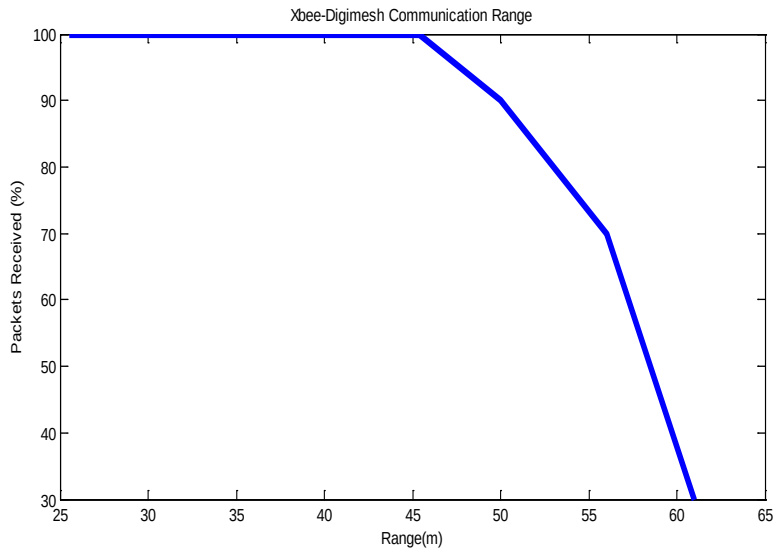

Figure 20: Percentage of packets received for different distances.

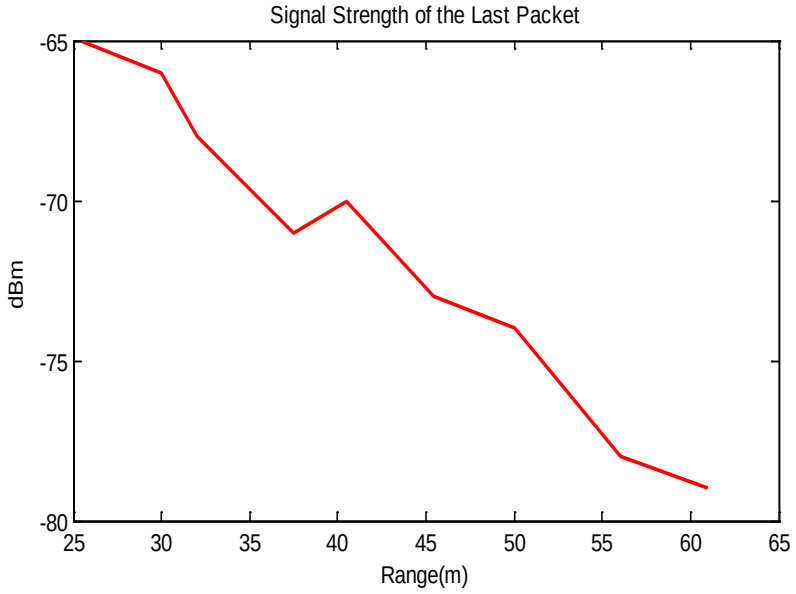

Figure 21: Signal Strength of the last packet.

4.3 ZigBee Transceiver Integration

A printed board with the Xbee chip was mounted on the microcontroller board. The pins of the chip for serial communication are connected to the digital input of the microcontroller (pin1,2); each serial data packet consists of a start bit, 8 bits of data, and a stop bit. In addition, pin 7 is connected to the output of the Doppler radar module. A LED was also added to the mounted board in order to indicate speed violation (with a pre-set speed limit).

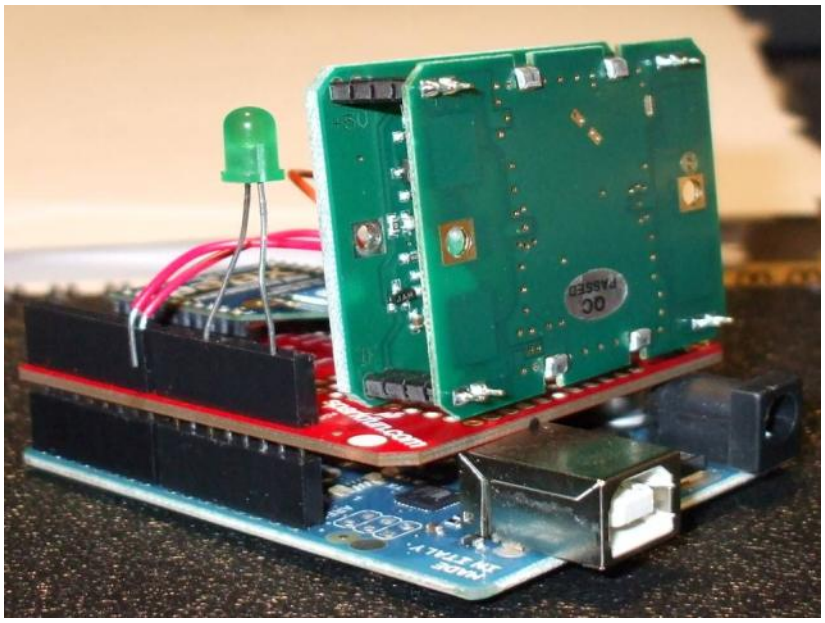

Figure 22: A more complete ZigBee test unit platform was assembled with the Doppler sensor on the top, and the microcontroller (MCU) board at the bottom.

The communication between the Xbee Digimesh module and the microcontroller was tested extensively both in lab and outdoor. For the low-cost node configuration, the microcontroller pools its digital input (pin 7) every 0.2 to 1 second (programmable) to count the number of pulses generated by the radar sensor, and sends the result to the Xbee Digimesh chip through the serial link (Figure 23). During the sensor tests, the speed data is transmitted to another Xbee module that is connected to a host computer.

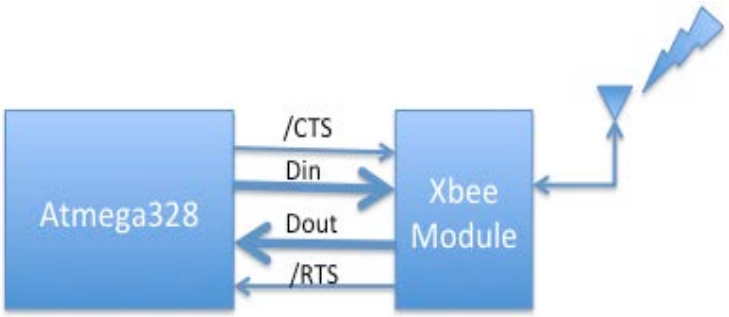

Figure 23: Serial link between the microcontroller and the Xbee module.

The lab testbed of the small radar sensor network contains three nodes (Figure 24).This includes node 1 (X or K band Doppler radar, microcontroller, Xbee module), node 2 (Xbee module, microcontroller), and Xbee router (Xbee module, computer).

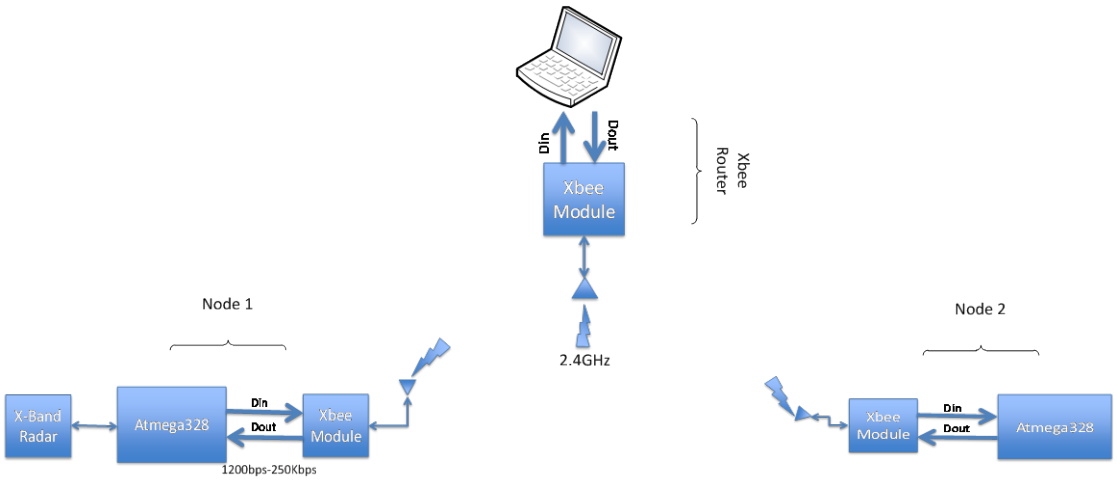

Figure 24: Wireless network diagram with ZigBee nodes.

Different software codes were written for each microcontroller, and one of the Xbee modules was configured as a router in order to test different topologies (Figure 25 and 26). Example topology 1: microcontroller 1 (source device) was programmed to stream data from the X-band Doppler radar to node 2 (remote device) through the Xbee router which is connected to a computer to monitor the values. Example topology 2: node 1 and node 2 streams data to the computer though the Xbee router. Example topology 3: computer broadcasts random values to node 1 and node 2. All of these topologies worked successfully.



Figure 25: Wireless network configuration during lab test stage: source device, router, and remote device.

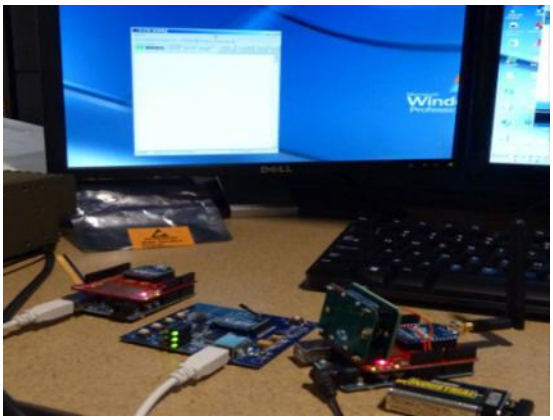

Figure 26: Testing of the network communication topologies.

4.4 Data Logger Incorporation

Data logger units are also incorporated into the transceiver modules for field deployment tests. The data loggers were installed in two different nodes in order to collect speed data from the Doppler radars. Each data logger node includes an Xbee Radio, a micro-controller, and a MicroSD card with 16GB of capacity which guarantees sufficient capacity for real-time data collection for several days, higher capacity options can be also considered. The logger shield includes a 32.768 KHz crystal, and a real time clock (DS1307) that keeps the time going even when the micro-controller is unplugged by using a backup battery (CR1220). The shield is connected with the Arduino micro-controller via the I2C protocol using pin number 4 and 5. Figure 27 shows the data logger shield with a SD card holder which has a 16GB MicroSD card, and the integration of the three elements is shown in Figure 28.

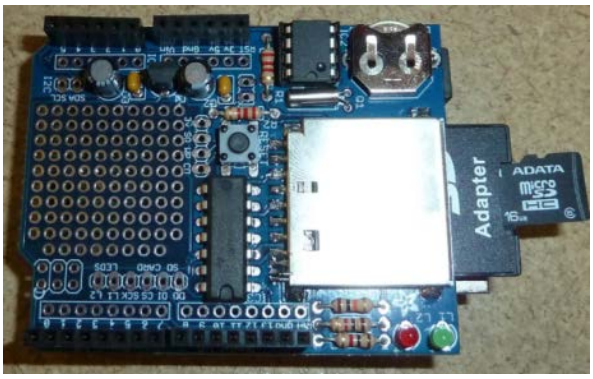

Figure 27: Data logger shielded with a SD card.

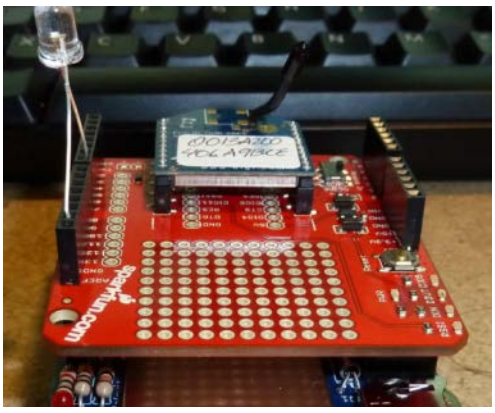

Figure 28: Data logger integrated into the transceiver module.

The critical issues of the ZigBee radio platform include weather-resistant integration and the software. More details on the software programs and network implementations will be discussed in Section 6. There are possible software protocol improvements for better node-flashing

synchronizations. An optimized software implementation will help to reduce the time delay, power consumption, and have better synchronization between nodes.

The latest version of the node software controls the LEDs' flashing rate, receive, collect, and transmit data from the radar. A flash memory interface is added, the speed values from radar detection can be saved as a text file in a MicroSD drive, which enables data collection and post-analysis in field experiments, each entry in the data file contains the corresponding date and time information in the following format: "mm/dd" and "hh:mm:ss".

5. The Radar Sensor Developments

5.1 X-band, Low Cost Doppler Radar Sensor

The first Doppler radar sensor tested in the project was a $10 X-band Doppler radar sensor. The miniature Doppler radar sensor was tested in the lab using an oscilloscope as analog interface, and human motion as target, as seen in Figure 29. As a basic function verification result, it is observed that the frequency of the sensor output does vary according to the target motion speed, in spite of the clutter environment in the lab.

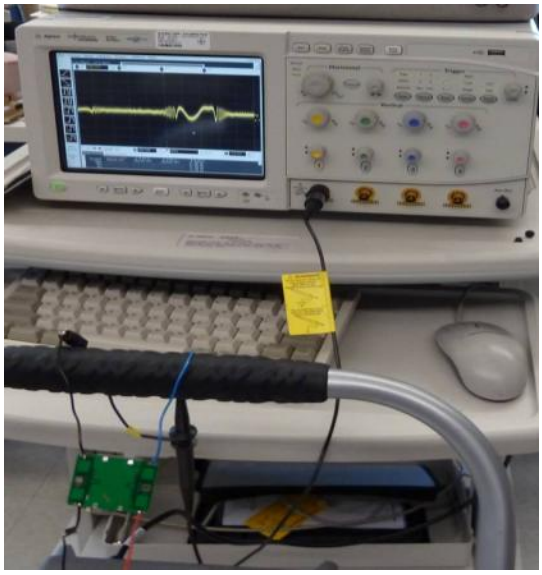

Figure 29: Lab test of the basic functions of a low-cost X-band prototype Doppler radar sensor.

As the laboratory tests show that intermediate frequency (IF) signal coming directly from the Doppler radar is weak when a target approaches from far distance, therefore, a low-frequency amplifier circuit was prototyped in the lab to boost the signal from the IF output of the Doppler radar. A breadboard circuit of this amplifier was built and the gain was carefully tuned. Using

Altium Designer software, the schematic and layout circuit was created for PCB fabrication, as shown in Figures 30-31.

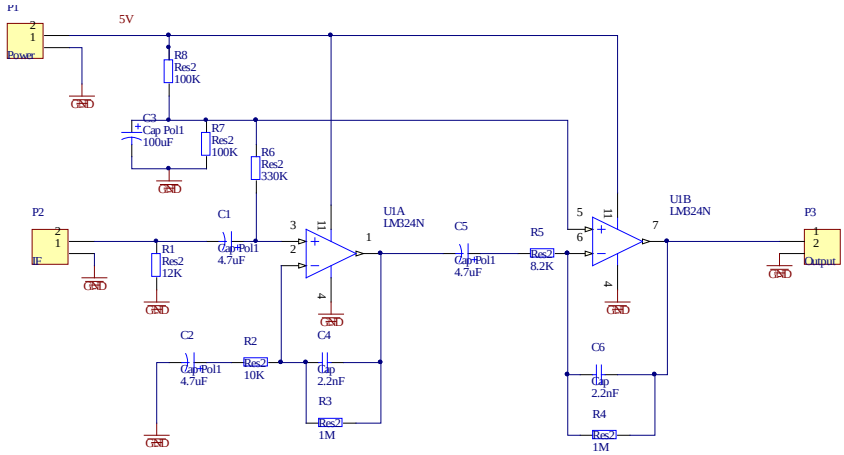

Figure 30: Doppler Radar Intermediate Frequency (IF) stage schematic circuit

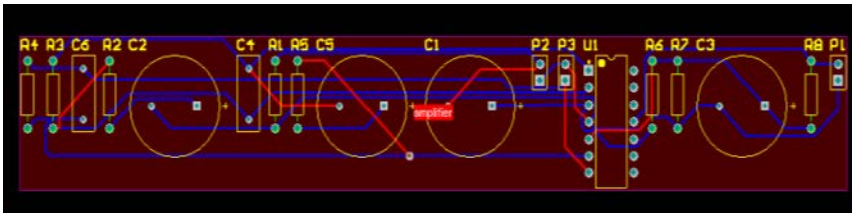

Figure 31: PCB layout

With Doppler sensor, breadboard amplifier and simple DAQ interface, target detection tests were done in RIL using different small targets; an ATMEGA328 microcontroller samples the amplifier outputs. Typical radar signature is shown in Figure 32, in which we can observe clearly how the frequency of the Doppler shift is proportional to velocity of motion.

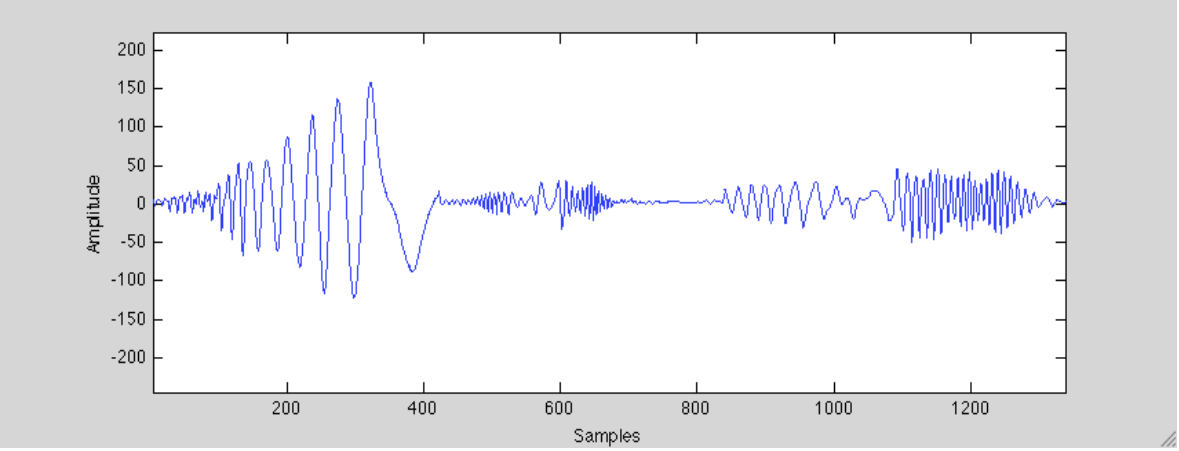

Figure 32: Doppler radar moving target signature recorded by the microcontroller.

In addition, a LabVIEW program on host PC was implemented to monitor the integration of the antenna, amplifier, microcontroller and Xbee module (Figure 33). Later, a new program for the microcontroller was implemented in order to establish the wireless communication between two embedded endpoints.

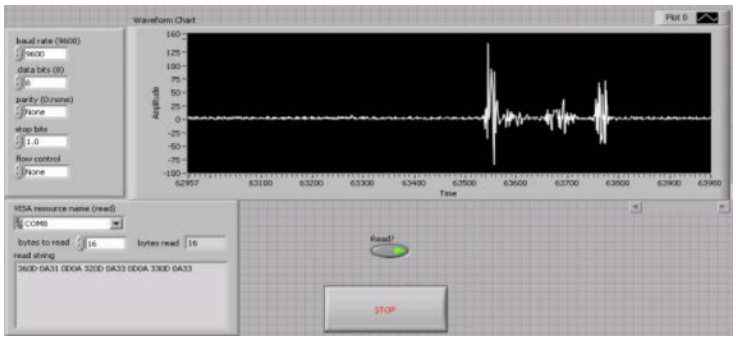

Figure 33: Developed real-time PC interface showing Doppler radar signal.

The Doppler sensor system was moved to a parking lot for an initial test. An oscilloscope was used as the real-time data observation tool, and we tested a car approaching with speed 30-50 mph (Figure 34). Some motion was detected from the scope displays. We then performed continued testing on the low-power Doppler radar sensor with sensitivity control circuitry and pulse number modulation (PNM) at output. From theoretical calculation and component datasheet, this sensor should be able to provide reliable speed indication for a mid-size car at up to 9 meter range, and the number of pulses generated per time period is proportional to the speed. However, the PNM output must be calibrated, as the speed estimation may not be accurate due to factors including the size of the car, antenna position, the range of vehicle (which lane it is placed).



Figure 34: Initial outdoor test of Doppler radar sensor.

We first did a parking lot test in South campus with Dr. Zhang's personal car, it was found that the sensor does detect the car as it passing by, but the speed indicator for single speed (i.e., 40 mph) has about 10 pulses in 0.5 sec sampling period, changing the antenna orientation does make a difference, which pointing the antenna beam perpendicular to the road yields the best detection sensitivity. Then the low-power Doppler sensor module (with MCU board) was moved to the roadside of High Way 9 in Norman for a test (Figure 36), where data was collected with the system working in two different modes: low sensitivity (lower amplifier gain), and high sensitivity (higher amplifier gain).



Figure 35: Initial setup of the radar sensor tests.



Figure 36: Collecting data on High Way 9.

In Figure 37, sample statistical results of the recorded traffic flow with the sensor module are depicted. The horizontal axis is time in seconds; the vertical axis is the number of pulses counted from sensor output. Note the sensor module is tuned to sample at each 0.6 sec for this test, so normally each sample with high pulse number represents one single vehicle (except when there are two vehicles in parallel on the road).

As the traffic is periodic, we can see clearly the 'quiet time period' in which there was no traffic on the road, and pulse count reading are all below 10. The average speed of traffic in highway 9 is 50-70 mph, which maps to 20-50 pulse counts for all kind of vehicles. There are few times the reading exceeding 70, which was caused by very large trucks. We also observe that there may be more false detections appear for high-sensitivity mode by comparing Figure 37 and 38.

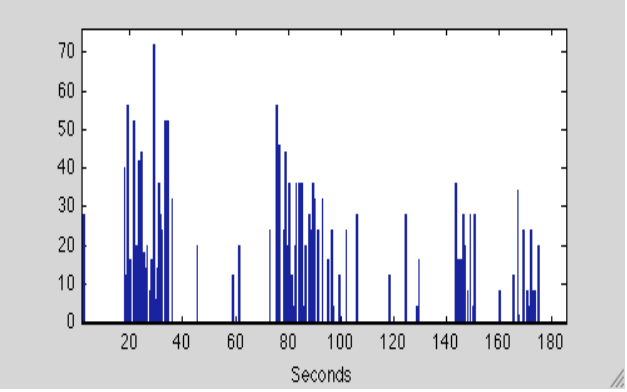

Figure 37: Sample recorded traffic data with low-sensitivity mode.

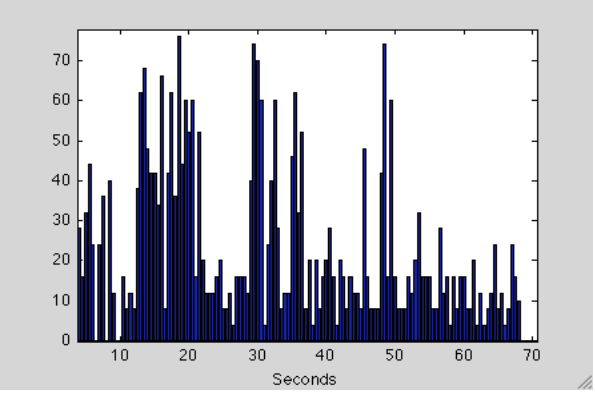

Figure 38: Sample recorded traffic flow data with high-sensitivity mode.

The conclusion is that the low-cost, low-power Doppler radar sensor does the job it is expected to, while more tuning and adjusting is needed in order to achieve optimal results. The speed estimation algorithm must work in a *statistical* fashion to overcome sensor fluctuations and errors, which is being investigated. Combination of low-power and higher-power Doppler sensors, adding more accurate radar sensors in the network, as we have proposed before, may also be a good solution.

5.2 K-band, High Quality Doppler Radar Sensor

In the final system integrations and field deployments, we incorporated a higher power K-band radar node from Huston Radar (http://www.houston-radar.com/). This sensor node just has relatively higher power than the X-band node, and also has long battery life. The higher unit cost for small quantity ($300-400 each), however, requires us to only use a few of them in the entire ZigBee sensor network. The specifications for this sensor are:

Table 2: K-band Doppler Radar Sensor Specifications

Frequency	**24.125 GHz.**
Polarization	**Linear**
Power Output	**5mW**
Antenna Beam Pattern	**45deg x 38deg**
Data rate	**1200 to 1152 baud**

The K-band Doppler radar system was placed along the side of Highway 9 in Norman (Figure 39 and 40), and vehicle speed data was collected for about 20 minutes.



Figure 39: Initial setup of the *higher power* radar sensor node.



Figure 40: Statistical traffic data collection setup on High-Way 9.

This sensor is well-calibrated and has longer effective range than X-band lower power radar. A LabVIEW interface was also implemented in order to collect (through serial port) and display in real-time the speed of vehicles passing by (Figure 41).



Figure 41: A LabVIEW interface showing recorded speed of vehicles.

The system was then configured to collect data only when incoming traffic is detected (record zero when there is no traffic). Figure 42 shows speed data recorded in this experiment, where the vertical axis is the speed expressed in miles per hour. Note the gaps among traffic streams have been removed as zeros. In this case, the average speed is 52.11 mph, while the minimum and maximum measured speeds are 33 and 68 mph, respectively. The 'spikes' in the data stream are good indication of speeding.

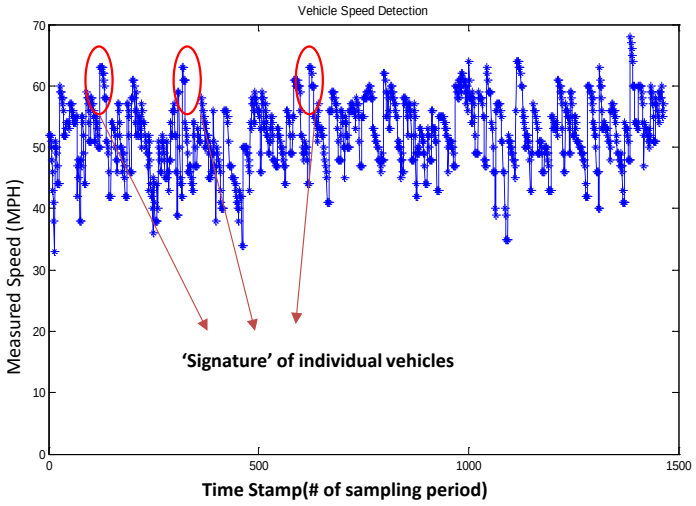

Figure 42: A snapshot of the statistical traffic speed data on HWY#9, based on higher power radar sensing node. The estimated radar data rate is 5-6 samples/sec.

We noticed that the radar is able to start detecting the incoming vehicles from about 70 meters, even though that distance also depends on other factors such as battery capacity, mounting height, pointing angle, etc. We also noticed that due to the relative geometry of antenna beam and incoming vehicle, the speed signature of individual vehicle tends to decrease during the observation time, as shown in Figure 43. The traffic in the adjacent lane may also cause some

level of interference. Choosing appropriate speed sampling period, good predication of radar signature durations, and the appropriate sensor installation has resolved such issues.

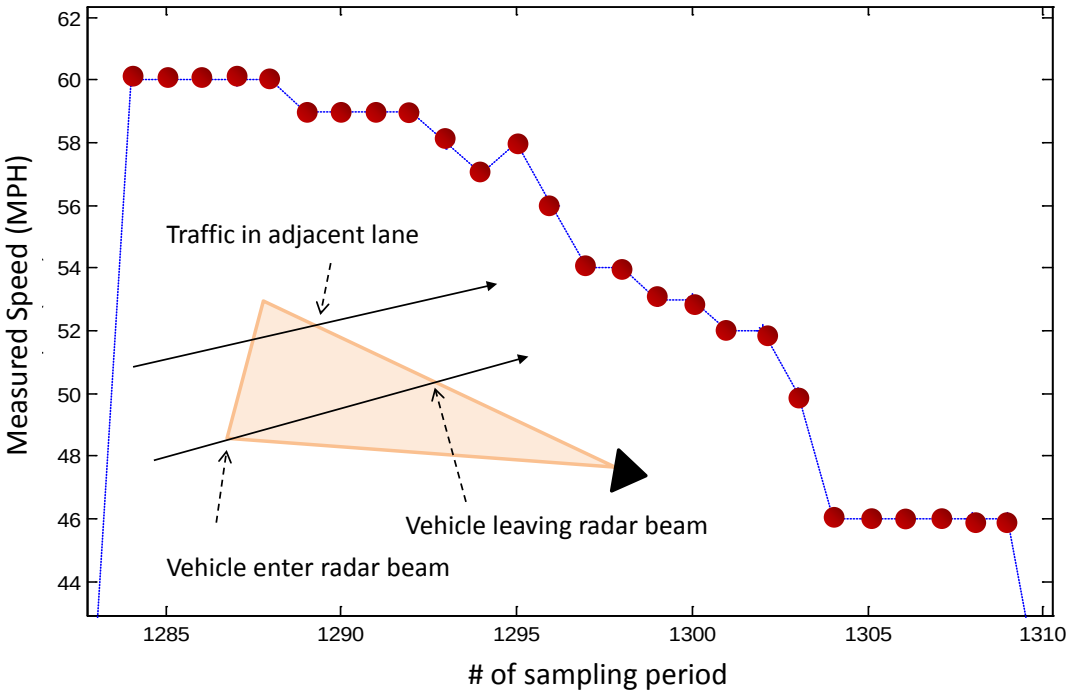

Figure 43: Measured speed data for individual vehicle tend to decrease with time as the vehicle leaves the radar beam, and the vehicles in adjacent lanes may have effects too.

The size and weight for the radar sensor were reduced and customized in order to allow installation in the interior of the warning LED light enclosure. An additional solar panel and backup batteries were used for ensure the radar sensor could continuously operate at least a week. Later, modifications in the circuit were done in order to have a single external power source input. From the field tests, the radar nodes using K-band radar sensor are proven to work effectively and reliably.

6. System Integration and Initial Field Deployments

6.1 Overview of the Prototype Smart Barrel System

An important task of this project is to actually demonstrate the concepts and technology of smart barrel system through a small-scale (about 10 nodes) system implementation and deployment.

As a small-scale prototype, we do not expect it is optimized in terms of power efficiency, reliability and product maturity. However, it should contain all the basic types of nodes in a smart barrel system network, and achieves the critical functionalities of traffic speed monitoring and warning.

The prototype system is composed of high-power and low-power nodes which include microcontrollers, radar sensors, XBee radios, LEDs and other electronic components. Figure 44 and 45 show the internal architecture of smart barrel nodes.

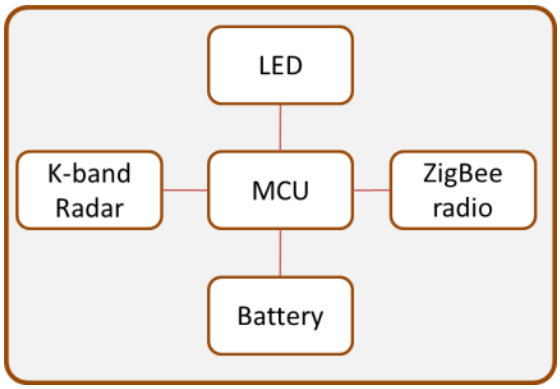

Figure 44: Smart barrel node internal architecture. The higher power (radar) node containing K-band radar sensor.

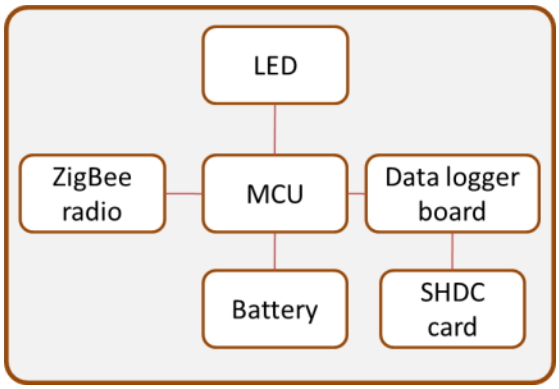

Figure 45: Smart barrel node internal architecture .The lower-power (radio) node with data logger. Data logger is not necessary for all the radio nodes.

For basic functioning, the prototype smart barrel system has been deployed as special type “B” lights (operating both day and night). A good depiction of nighttime operation is shown in Figure 46 and 47, the warning lights start to flash when speeding is detected, and the rate of flashing is

proportional to the detected speed (Figure 47). Otherwise, they are in “dim” mode and look like normal type “A” lights (Figure 46).



Figure 46: Warning lights in dim mode at night when no speeding is detected.



Figure 47: Warning lights flashing when speeding is detected.

In the following sections, we will describe the wireless network configurations, software implementations, the process of nodes integration, site selection and arrangements, and the field data results.

6.2 Network Configurations

Two simplest network configurations were programmed into the ZigBee radio nodes. The first configuration (Figure 48) is based on small-scale networks with a determined number of nodes, where the higher power radar nodes *broadcast* speed data to the other (radio) nodes. The advantage is better synchronization among the nodes within a section, and more flexibility to

arrange the low-power nodes along the work-zone. The disadvantages are the dependence of each network section on the radar sensor nodes, so the nodes in a section can stop functioning if the higher power node is down. Also as a broadcasting mode, the power consumption among the nodes is not balanced (i.e., the radar sensor nodes consume much more power than radio nodes so can become the bottlenecks of the battery life).

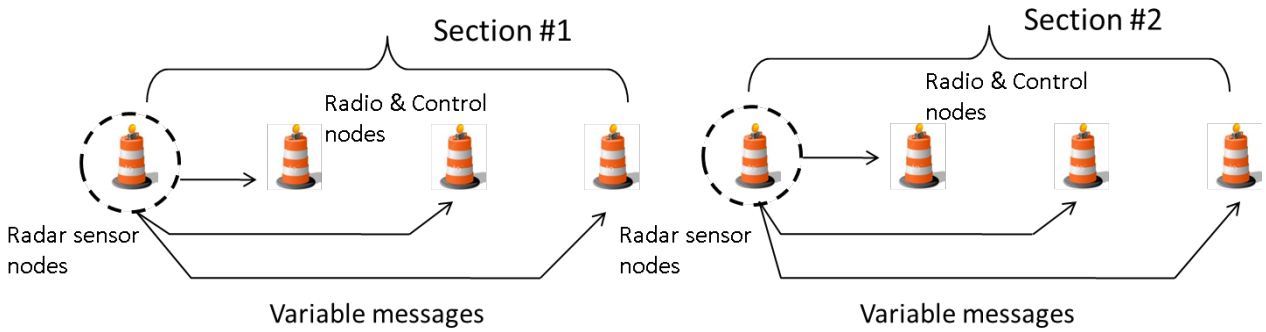

Figure 48: ZigBee Network configuration #1

In the second network configuration (Figure 49), a unique address is assigned to every node which recognizes the adjacent nodes and updates its routing table constantly. In this configuration speed data is transmitted sequentially to the other nodes, and each node adjusts the LED flashing rate based on the message received and its local computing. This configuration needs less high power nodes, achieves better messaging reliability, and better power consumption balance in the network. The number of radio/control nodes in a section can be larger than that of the first configuration. However, it still has dependence on the radar node, and the time delays during sequential messaging can affect the synchronization of the nodes.

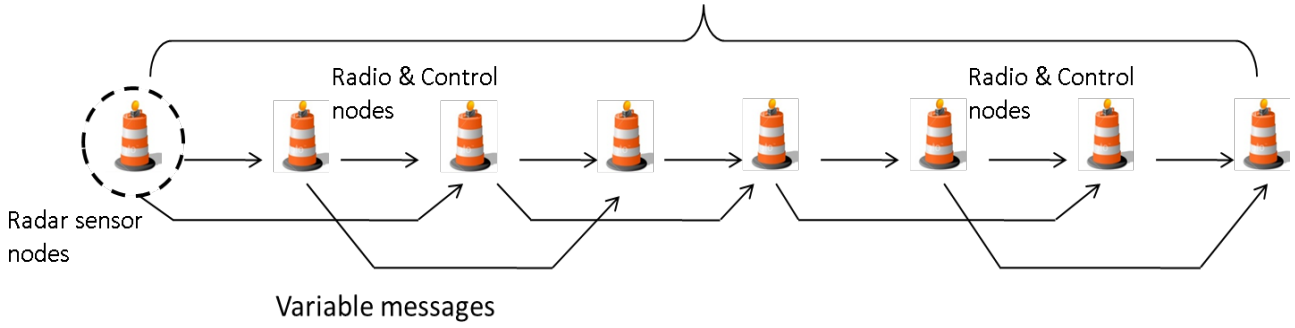

Figure 49: ZigBee Network configuration #2.

Considering its simplicity and initial demo requirement, the first configuration is used in field deployment and data collections of this project.

6.3 Software Implementations

An embedded C-program was developed and downloaded to all the microcontrollers of nodes, which implements the ZigBee-based wireless communications among the smart barrel nodes, and performs speed computation as well as warning message decisions. Specifically, this program can process/storage speed data in real-time, ensure synchronization among the nodes, and control the LED's flashing rate. The general flow diagram of the program is shown in Figure 50.The program starts by setting up the constant values for speed limit, intensity of brightness, and parameters such input/output digital ports, UARTs configuration code is set as 9600-N-8-1 (9600 baud, 8 bits, no parity, 1 stop bit),SPI interface, buffer size, and timers. The MCU identifies what type of network the system operates with by checking the status of a digital input pin or a software variable.

When a data packet is received through the serial port, the MCU reads the buffer and converts the raw data bytes into speed values (in unit of mph), this value is needed to calculate the LED flashing rate, which ranges from 4 to 20 (flashes/second), speed and flashing rate are related by the following equation:

$$N = 2000/(a - b \times Sp) \quad (1)$$

Where *a*, *b* are constants values, *S*p represents the detected vehicle speed, and *N* is the flashing rate (flashes/second). For this project we are considering *a*= 500, *b*=4. For example, for a vehicle speed of 100mph, the LEDs flash at a speed of 20 times per second.

If the node includes a data logger, speed values from radar detection will be saved as a text file into a MicroSD drive, which enables data collection and post-analysis in field experiments, each entry in the data file contains the corresponding date and time information in the following format: month/day(mm/dd) and hour:minute:second (hh:mm:ss).Depending on the network configuration, the MCU will choose to transmit to the next node or broadcast to the others nodes the speed values. If the speed value is higher than the speed limit, the LEDs will start flashing, the input variable for this function is the flashing rate in order to change the LEDs status 'N' times from on to off or vice-versa. Otherwise, the LEDs will remain in dimmer mode which is based on a pulse width modulation (PWM) function. In the first stage of the project a function to display the speed in a matrix of LEDs with different colors was also implemented (Figure 54 and 55).

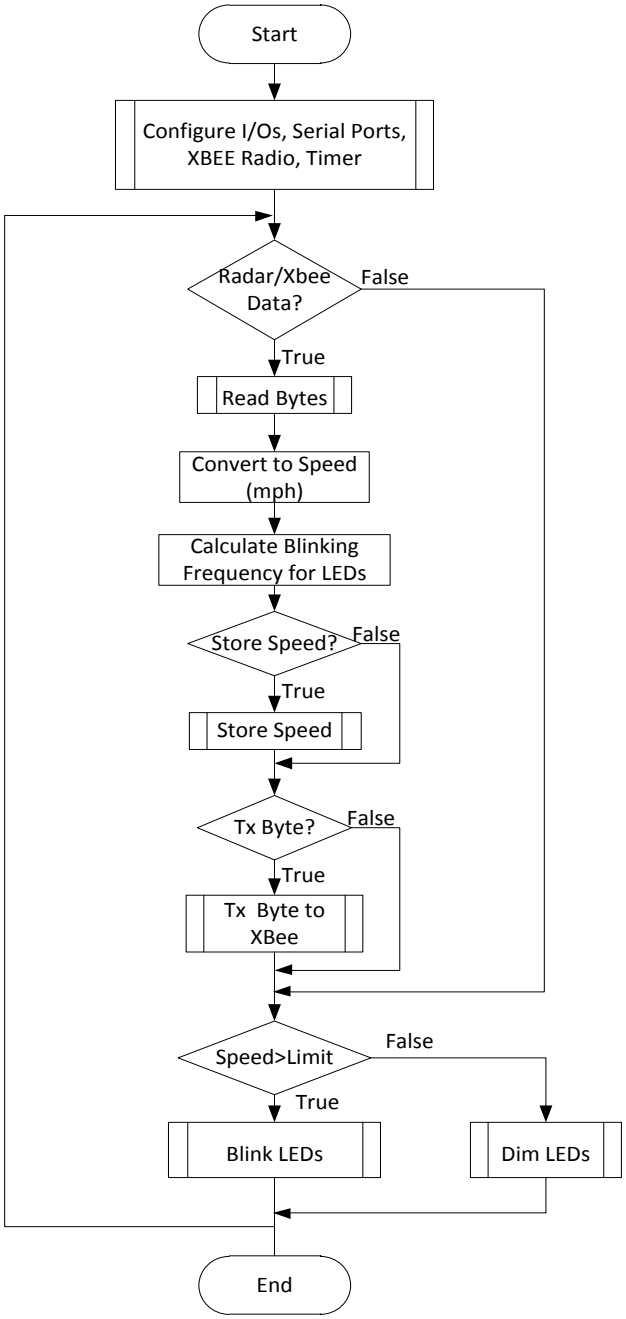

Figure 50: General Flow chart for data handling and LEDs control in each node.

6.4 Node Integrations

A sample traffic barrel was acquired (Figure 51) to mount and test our first integrated sensor and electronics, a simple program to process real-time data from the radar sensor was implemented in the microprocessor and tested in lab. This program transmits and receives

to/from other endpoints through the XBee wireless transceiver, and controls the traffic warning signal (LEDs).

For testing purposes, we initially used a matrix of RGB-color LEDs as traffic warning signal, which can be configured to flash in different colors. This peripheral interfaced with the microcontroller through the SPI interface. The node elements were installed onto the barrel as shown in Figure 51.

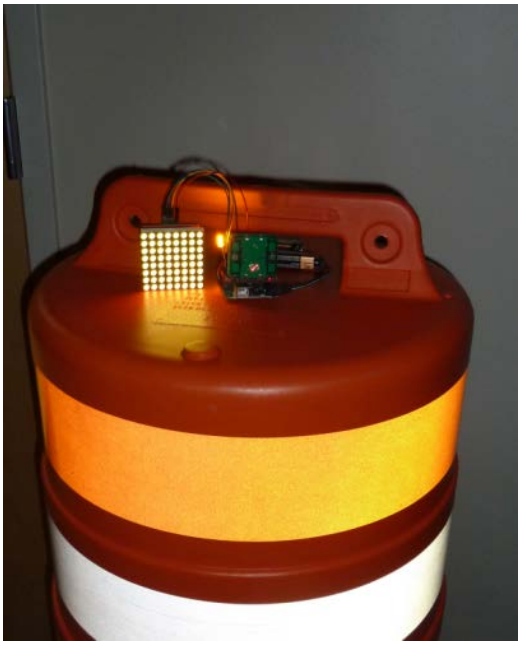

Figure 51: Initial system integration on a sample barrel: it includes the X band low-power sensor, Arduino Uno microcontroller, XBee module, and RGB LEDs.

Integrating the K-band radar sensor in the module was a little more difficult. The problem mainly originates from the fact that the microcontroller is not originally used to interface the data ports from the K-band radar. A CMOS voltage level shifter circuit was tested, but the result was not satisfactory. We then designed and fabricated an external RS232 to TLL voltage level converter circuit, which managed to integrate the K-band radar data ports to the Arduino Uno microcontroller, as is shown in Figure 53. Moreover, in order to synchronize the K-band sensor and the XBee module with the microcontroller, it was necessary to employ a microcontroller with two dedicated serial ports because of the timing issues with soft serial ports.

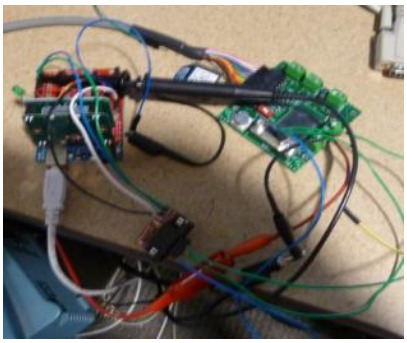

Figure 52: Testing a CMOS voltage level shifter circuit.



Figure 53: RS232 to TLL voltage level converter circuit.

The speed alert function were added to the laboratory system integration, the low-cost RGB matrix of LEDs can display the speed detected by the radar sensor, digits are shown in green color if the moving object does not exceed the pre-configured speed limit. As an example, if the speed limit is exceeded, the sensor node will show the digits in red color as we can see in Figure 54 and 55, where the speed of the moving object is 15 mph, higher than the pre-configured speed limit of 10 mph. The LED array was fully controlled to display any number, character, color and flashing frequencies.

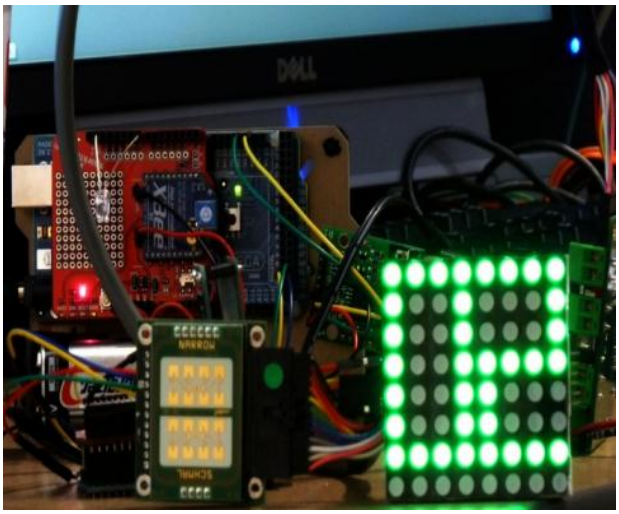

Figure 54: The RGB matrix of LEDs shows speed in green because the moving objective lowers than the pre-configured speed limit of 10 mph.

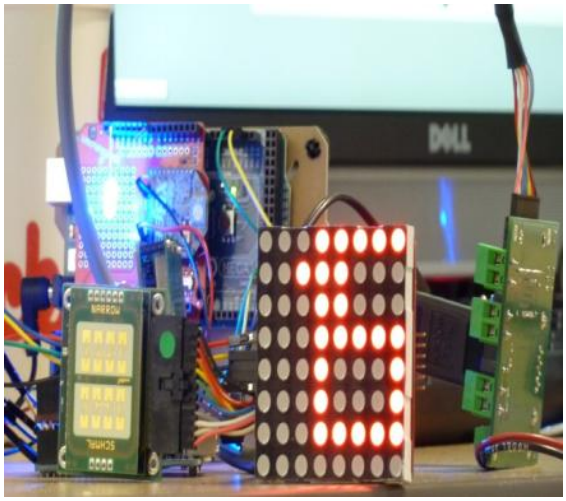

Figure 55: The RGB matrix of LEDs shows speed in red because the moving objective exceeds the pre-configured speed limit of 10 mph.

A temporary mechanical housing for each node was designed and built; it included a plastic enclosure and acrylic plates. As it is shown in Figure 56 and 57, sensor and digital display are on the plate, while the microcontroller, the XBee radio, and the battery are in the plastic enclosure.

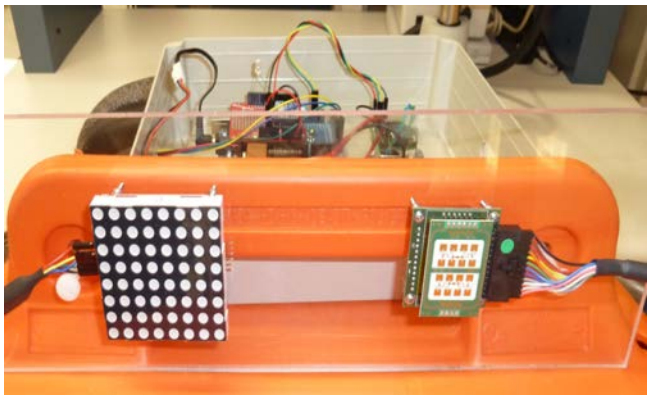

Figure 56: Mechanical housing for the high-power node.



Figure 57: Mechanical housing for the low-power node.

Using this temporary housing, a high-power and two low-power nodes were assembled. The high-power node was mounted on the top of the barrel and the other two on tripods, as shown in Figure 58.



Figure 58: Mounting of the three laboratory prototype nodes.

An important step toward the networked operation was achieved by testing a “multi-node” sense and display configuration. This small network included four nodes, node1: a K-band radar sensor, a microcontroller, LEDs, and an XBee radio. Node2 and node 3: a microcontroller, LEDs, and an XBee radio. Node 4: an XBee radio, and a laptop. The network configuration diagram is shown in Figure 59. Node 1 streams the detected speed values by the K-band Doppler radar to node 4 through both node 2 and node 3, then those values were displayed in real-time in node 4 where a LabVIEW program was running on it.

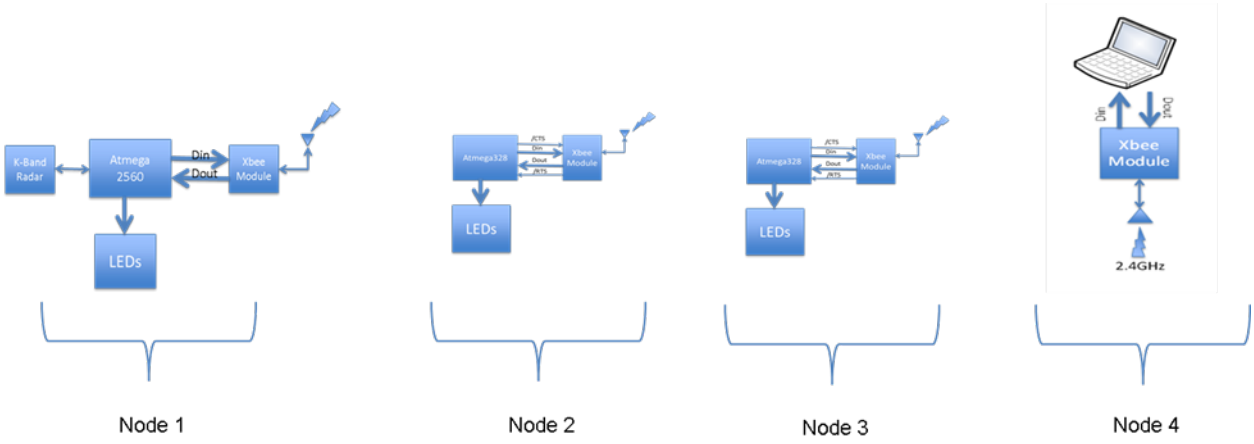

Figure 59: System configuration with four nodes.

After a successful testing of functionalities of the small network in the lab, the ZigBee nodes were placed along the roadside of Highway 9 to observe the behavior of the system under

actual traffic conditions, Figure 60, 61, and 62 show pictures of the highway test and node installations.



Figure 60: View of the zone.

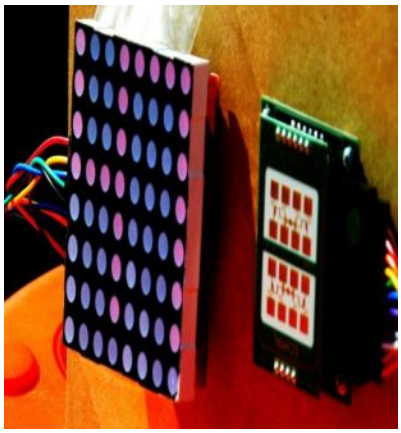

Figure 61: Higher power node.



Figure 62: LabVIEW interface registering speed data.

For the low-cost LED lights, at the beginning we considered using the blue color (Figure 63), but this color is not very common in the market. Instead, we chose the amber color, as it is still listed in the MUTCD standard as the color for the barrels. Traffic warning lights are normally classified into 3 types: A, B, and C. For this project, type “B” (high intensity) is the suitable option because during day and night the flashing of the LEDs has to be clearly distinguished by the drivers. Moreover, the necessity of reducing size and weight of the nodes encourage us to search for an appropriate warning light enclosure in order to accommodate all components. Enclosure structures from different manufacturers were evaluated before acquiring the type-B warning lights from Solar Masters, but some additional modifications were still necessary. Basically, we have redesigned or modified the mounting structures, LED driver circuits and control circuits of the Solar Master lights (Figure 64).

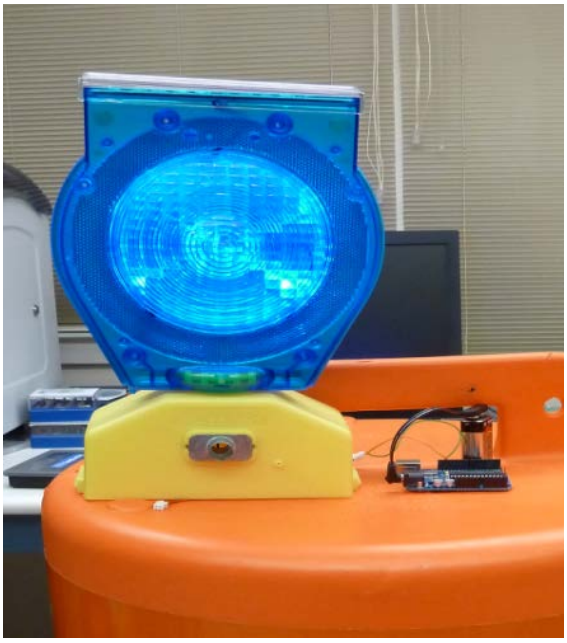

Figure 63: Type-A blue warning light

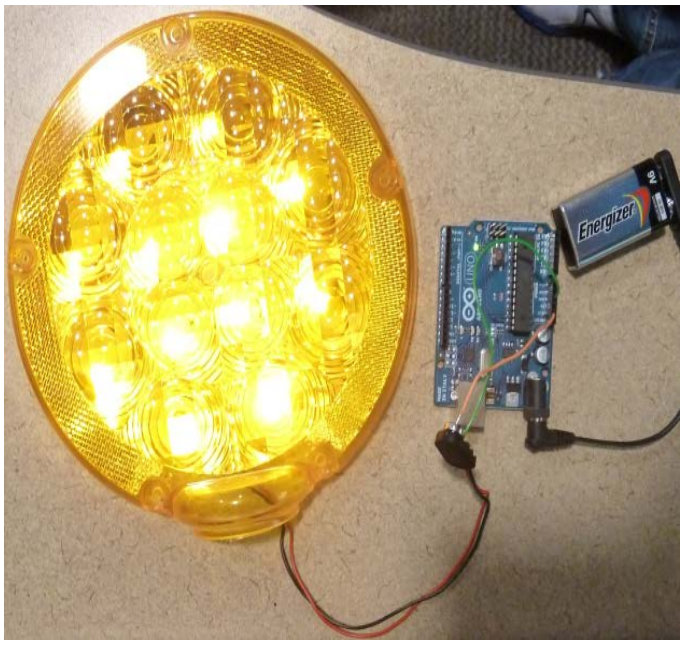

Figure 64: Type-B amber warning light.

The microcontroller board, XBee radio, and radar sensor were tested and integrated into the warning light enclosure as it is shown in Figure 65 and Figure 66 and 67, respectively. Each unit also includes a “master” switch to power on/off the components, and a solar panel with a rechargeable battery were used for the first work-zone field test, for further tests it is reduced to a single external power source input as the external battery has provided sufficient power to the expected test period.

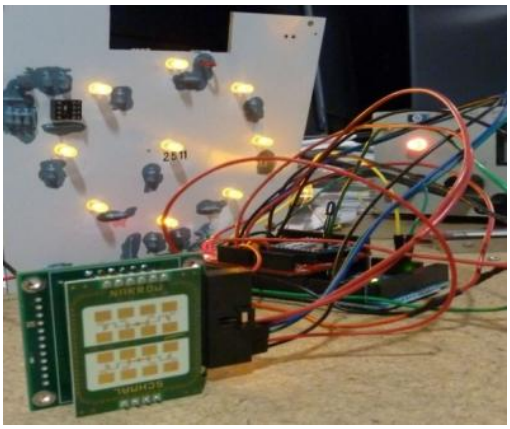

Figure 65: Interfacing radar sensor, microntroller, XBee radio, and LEDs.



Figure 66: Low-power node integrated with a solar panel and a rechargeable battery.

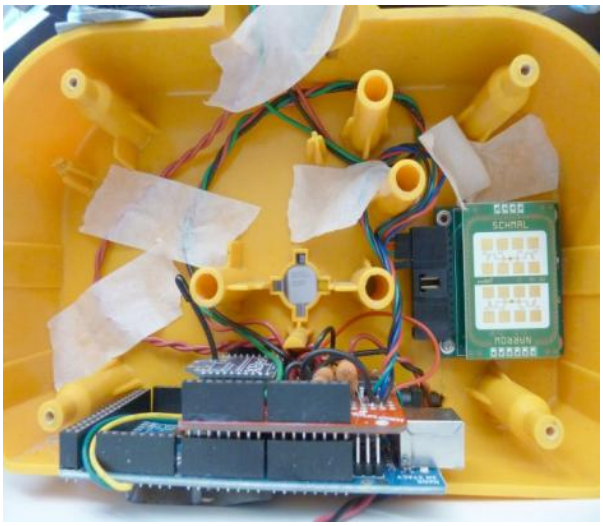

Figure 67: High-power node integration.

A new PCB board (Figure 68), on which a microcontroller and an XBee radio are incorporated together, was designed for next-stage integration, and to save power and space. MCU's and radio's serial ports are connected each other to allow data transfer among the nodes, a 16MHz crystal oscillator for the MCU and a power regulator circuit for the radio were also included. After successfully testing a prototype of the new design, the new PCB boards were sent for fabrication, and they worked as expected.

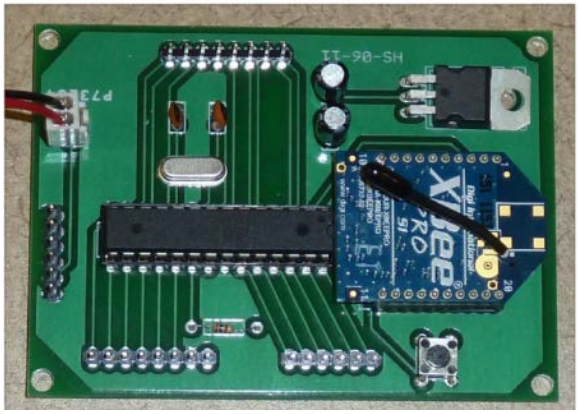

Figure 68: PCB board includes a MCU and an XBee radio.

Data logger shields were also incorporated into the system (Figure 69). They were installed in two different nodes to collect speed data from the K-band radars. Each data logger node includes an XBee Radio, a micro-controller, and a 16 GB MicroSD card, which guarantees sufficient capacity for real-time data collection for several days. The logger shield includes a 32.768 KHz crystal, and a real-time clock (DS1307) that keeps the time going using a small backup battery (CR1220), even when the micro-controller is unplugged. The shield is connected with the Arduino micro-controller via the I2C protocol using pin number 4 and 5.

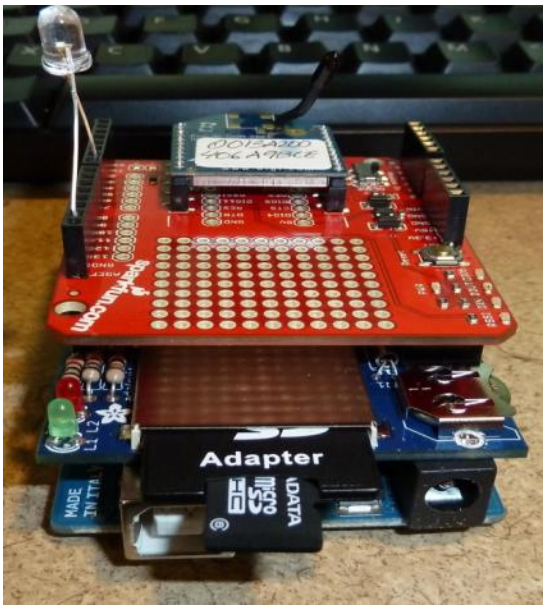

Figure 69: Data logger shield with a SD card holder which has a 16GB microSD card.

The implementation of the 10 boards was accomplished in mid-2011. All nodes were successfully programmed, and tested with two different topologies, the first one was to broadcast speed values from the K-band radar to all the rest of the nodes, and the second one

consisted of passing the speed values sequentially from one node to the next node, and so on. Each board was labeled with its unique Xbee radio address to facilitate programming and installation. Figure 70 shows the 10 modules when they were produced. Figure 71 shows the LED lights when the node electronics are incorporated.



Figure 70: The 10 programmable modules labeled with their respective address.



Figure 71: The 10 warning lights ready to be mounted on the traffic barrels.

6.5 Field Deployment Arrangements

An initial field deployment of smart barrel prototype is an important aspect of the system integration and evaluation. We considered several different deployment sites including some places in Norman, OK and a site close to OKC. Under the guidance of Mr. Westlund, the team finally selected a site on I-40, through working with Steve Burke in the Action Safety and Jeff Allen at the Allen Contracting for the test site at I-40 and Morgan Rd. The work-zone site is along the left side of I-40 highway driving from W to E, and close to the intersection with W Reno Ave (Figure 72).



Figure 72: Deployment zone location: 35°28'00.41" N 97°43'19.79" W. Warning message board: "flashing light ahead if speeding".

Two small networks were deployed at the selected workzone. The elements of network 1 are the nodes from 1 to 8, and network 2 is composed of node 9 and 10. The ten nodes were arranged along the highway using the site layout shown in Figure 73 where node 1 and 9 are the high-power nodes which include a K-band radar sensor. Data loggers are node 2 and node 10, each one includes a 16GB mini-SDHD memory card. A laptop, or a mobile node, is used to monitor the network interoperability. The normal standard of workzone barrel deployment was followed, with a separation of 50ft between adjacent nodes.

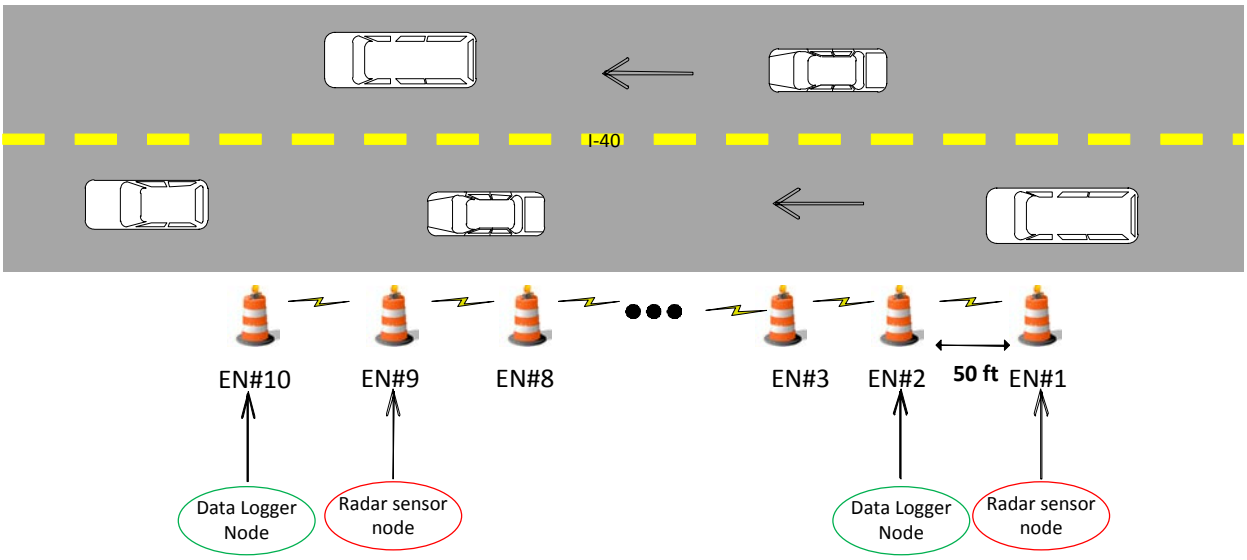

Figure 73: Deployment of the nodes along the construction site.

6.6 Speed Monitoring Data Records and Analysis Results

6.6.1 Field tests and data collection on Aug 28, 2011.

The initial deployment of the layout was accomplished on August 28th. Figure 74 and 75 show the pictures of this first deployment. During this test, an external solar panel and a 12V backup battery were used for the high-power nodes. The solar panel was mounted on the top of the barrel using some screws; the 12V battery was set up in the interior of the drum. For the other nodes, all the components were integrated inside of the enclosures to make easier and faster deployments. All the lights were successfully deployed, they flashed as programmed when a speeding vehicle was detected.



Figure 74: Team deploying the warning lights during daylight

After three days of the installation, we were reported that some nodes were not working properly, during the night of Aug 31, we went to check out the system, and found that some nodes were off because of low-batteries. The high-power nodes using solar panel were still operating normally as shown in Figure 75. Four of the nodes with battery issues were brought back to lab for inspections, and they were temporally replaced with normal drum lights.

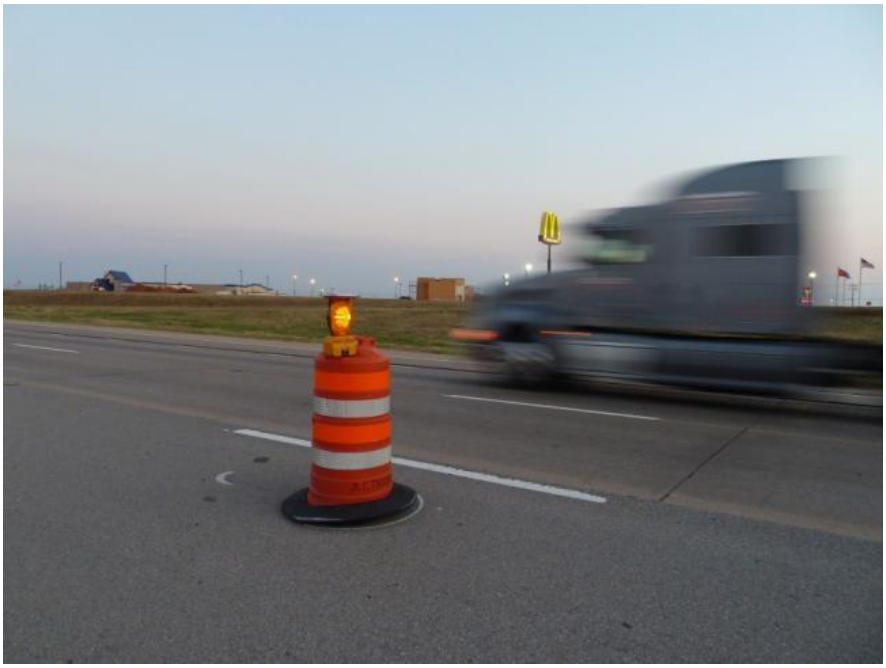

Figure 75: High power node was still working after three days of the installation.

Data collected from each high power node was analyzed. There were some software issues on the date/time recording so the data recorded in this test has no time stamps. Figure 76 and 77

show the first 100 minutes (18000 samples) of "continuous" traffic data, for the first node we found that the mean speed value is 61.153 mph, and the standard deviation (STD) is 4.816 mph.

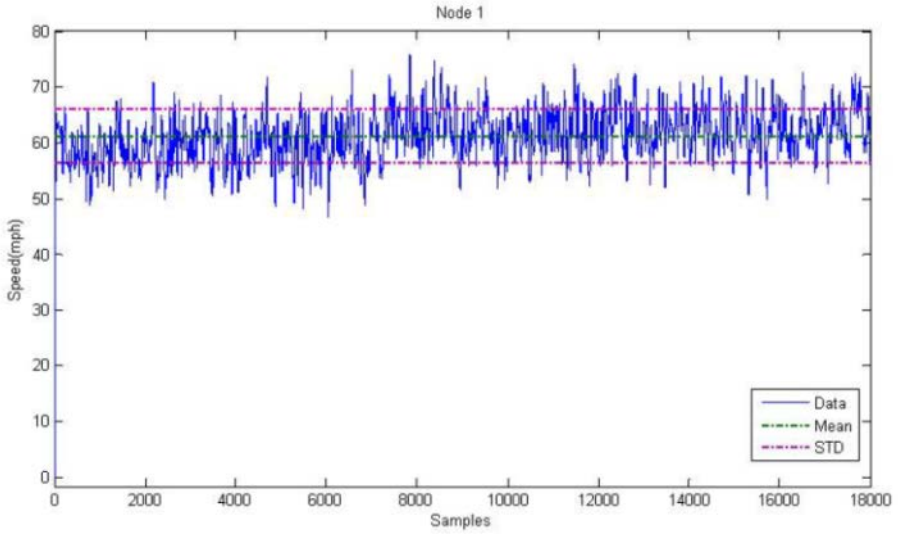

Figure 76: Plot of the first 100 minutes of continuous data. Mean speed= 61.153mph, and STD= 4.816mph.

For the second radar sensor, the measured mean speed is 60.42 mph, STD = 3.44 mph, we can also observe that the speed decreased during an interval of 30 minutes, which could be related to our team's presence while installing the lights along the highway.

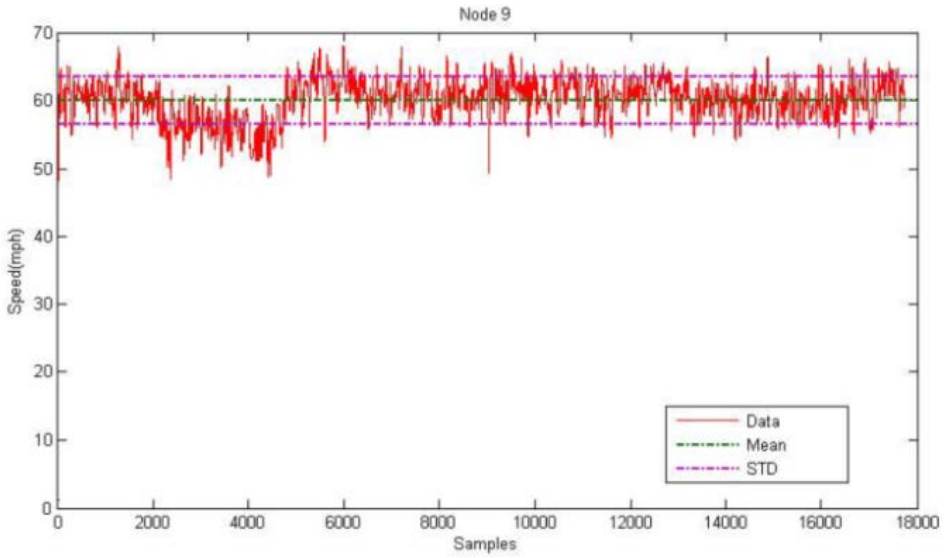

Figure 77: Plot of the first 100 minutes of continuous data. Mean speed= 60.42mph, and STD= 3.44mph.

In Figure 78, the complete data set collected by node 1 is plotted, it contains 180000 samples, which represents 16.6 hours of "continuous" traffic data. Note as the actual traffic may be intermittent, the actual operation time is longer than that. The mean value is 61.48 mph, and the STD is 3.92 mph. We can also observe that the speed is under the mean value for a specific period of time, it could represent some traffic slow-down during the day. The second data logger node run out of battery power earlier, so the usable length of "continuous" traffic data is about 100 min.

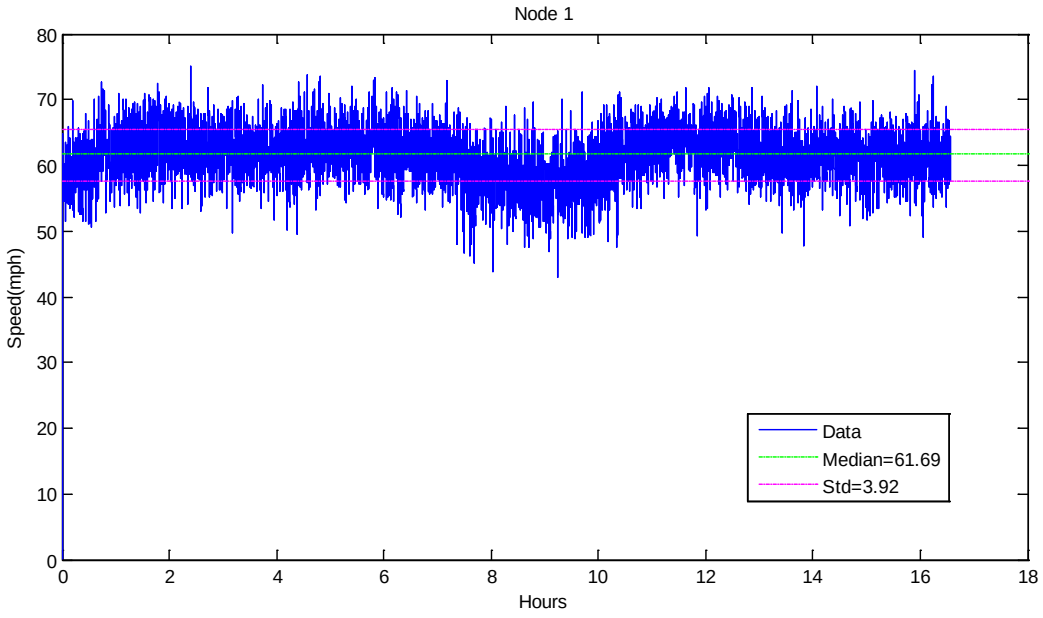

Figure 78: Plot of 16.6 hours of continuous data. Mean speed= 61.69mph, and STD= 3.92mph.

Although the initial records did not contain enough data to evaluate the effectiveness of this system, there were indications of promises that it can be easily more effective if the nodes run longer period of time, has larger number of nodes deployed, and work together with other warning methods. Mr. Chris (in Action Safety) suggested we should consider changing the light color to blue to others to enhance the impact of alarm.

6.6.2 Discussion of the initial deployment data results until end Sep 2011

Data collection continued throughout Sep 2011 and there were some technical issues to have both data loggers (for radar 1 – entering the zone and radar 2 – existing the zone) working at the same time. However, interesting and important observations can be made on the data records from this period, which are depicted in Figure 79, 80 and 81. Firstly, if we compare Figure 79 and 80, we can see the average traffic entering the smart workzone has quite

constant average speed (about 5 miles above the speed limit) and does not get affected by the change of flashing speed of LEDs. Also, it is obvious that the traffic speed is slower during the night-time (until 7-8AM), and then gradually build up speed during the start of work hours. There is no firm conclusion that the traffic slow-down during nighttime is due to the smart barrel signals, but it is true that the lights are more effective during nighttime than during daytime.

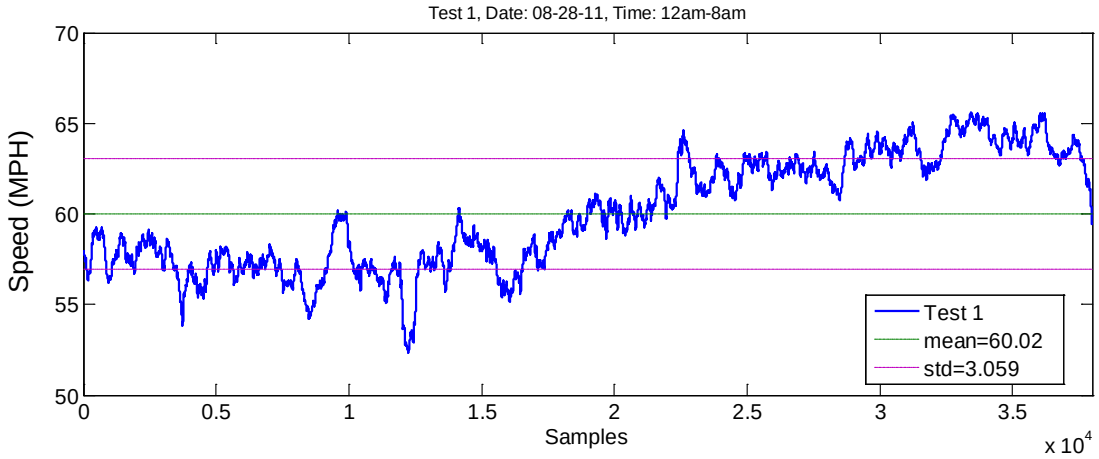

Figure 79: 8 hour traffic Aug 28, low-flashing Rate, entrance of zone

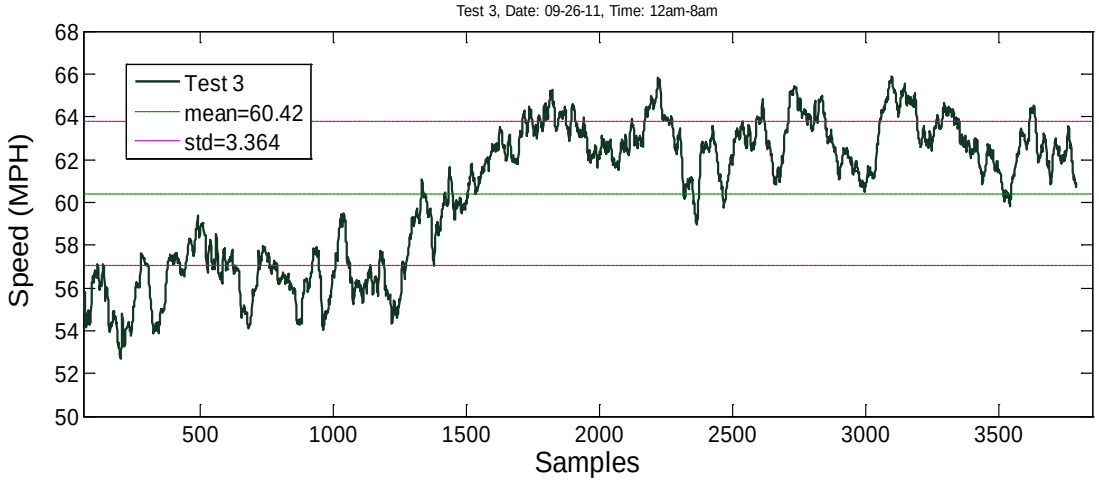

Figure 80: 8 hour traffic Sep 26, high-flashing Rate, entrance of zone

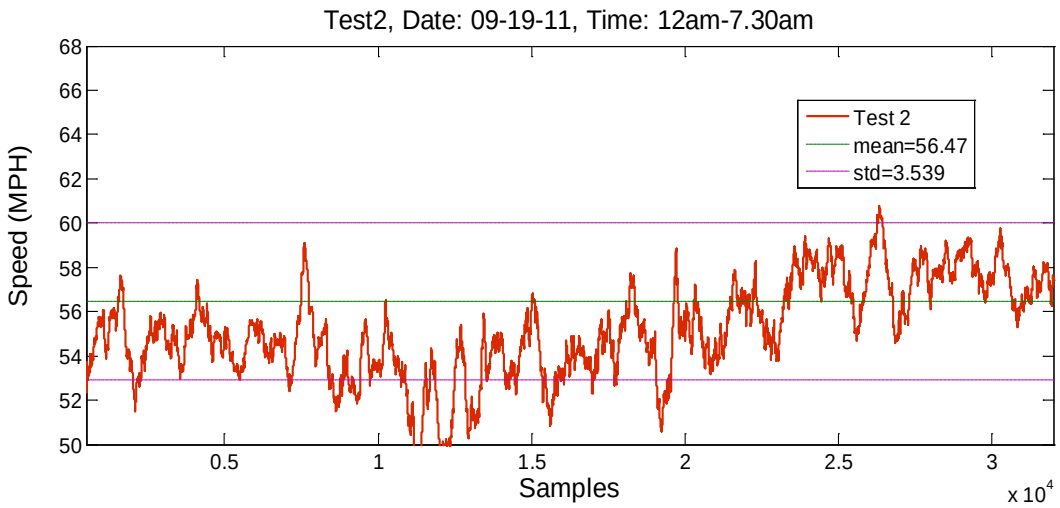

Figure 81: 7.5 hour traffic Sep 19, high-flashing Rate, exit of zone.

Comparing the speed entering the smart barrel zone and leaving the zone (Figure 79, 80 and 81), it is seen that the average traffic speed is reduced by almost 5 MPH. Again, since data from (79)-(81) is not from the same time period, it is not very clear if this is completely due to the deployment of the smart barrels, but it is indeed another promising indication of the effectiveness of the smart barrel system.

6.6.3 Oct 2011 data record and analysis

Prior to performing this test in Oct, we had evaluated the performance of 6V batteries in simulation with two nodes and blinking the LEDs with different flashing rates for at least 72 hours. In terms of battery life, the simulation results were in accordance with field observations. Modifications in the circuit were done in order to have a single power source input. From the field tests, these radar sensor nodes are proven to work effectively and reliably.

In these records, data from the first radar (upstream, entering the workzone) is considered as the traffic speed stream before entering the smart barrel zone. Data from the second radar (downstream, leaving the workzone) is considered as the traffic speed stream in the middle of the work-zone. In the first week of October, a test was performed on the I-40 site, some results were presented at the "2011 ODOT-PkTC Transportation Research Day". Figure 82 shows data collected from the first radar sensor during the second test, the flashing rate of the lights were increased, and the new 6V batteries make the lights brighter at night. In Figure 83, speed data from the same time period and same LED configuration is shown from the second radar node. There is a clear indication of speed reduction comparing Figure 82 to Figure 83. Same conclusion can be reached by comparing another time period (Figures 84 and 85).

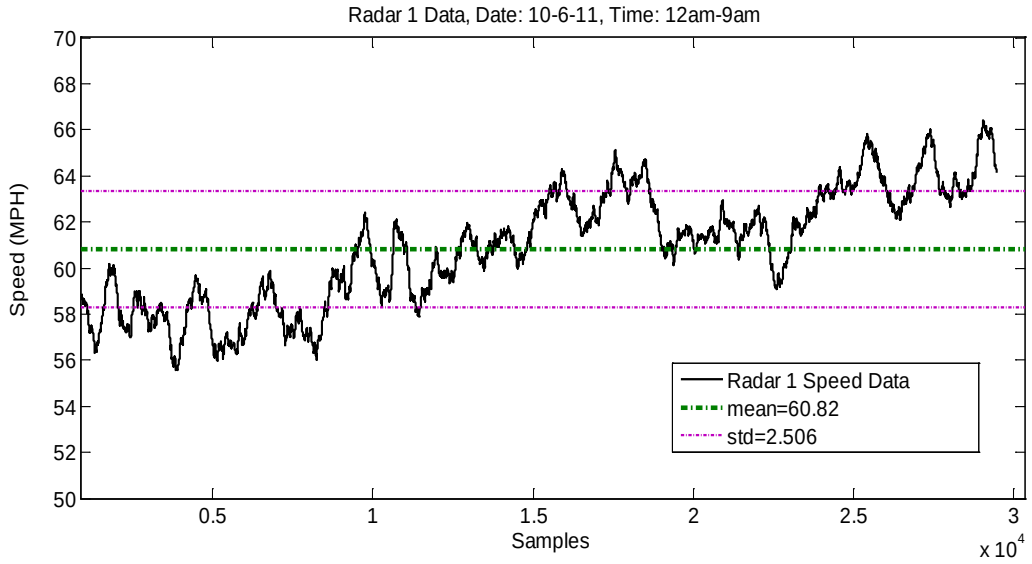

Figure 82: Oct 6 data – Radar 1: 12 AM -9AM.

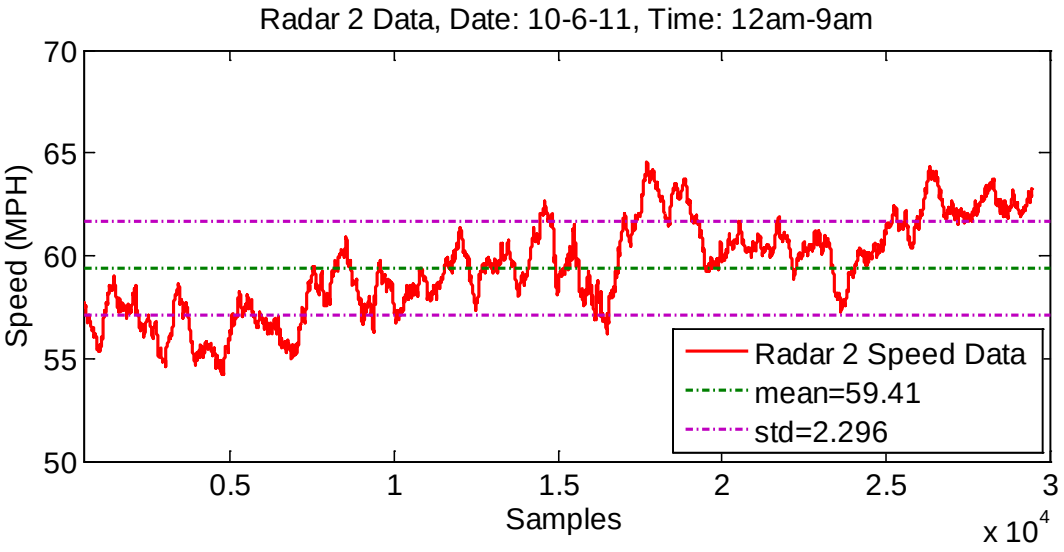

Figure 83: Oct 6 data- Radar 2: 12 AM-9AM.

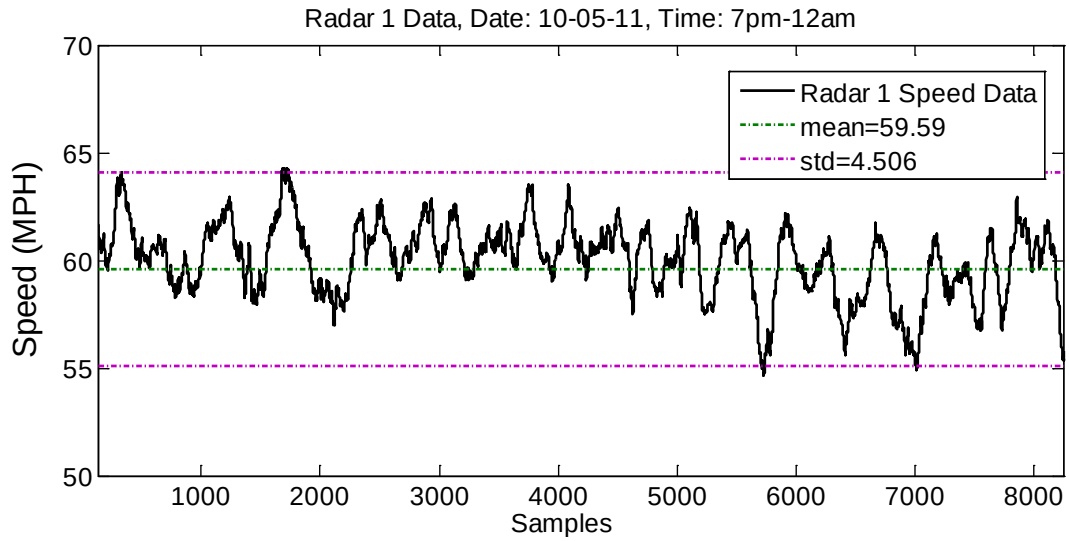

Figure 84: Radar 1: 7PM-12AM.

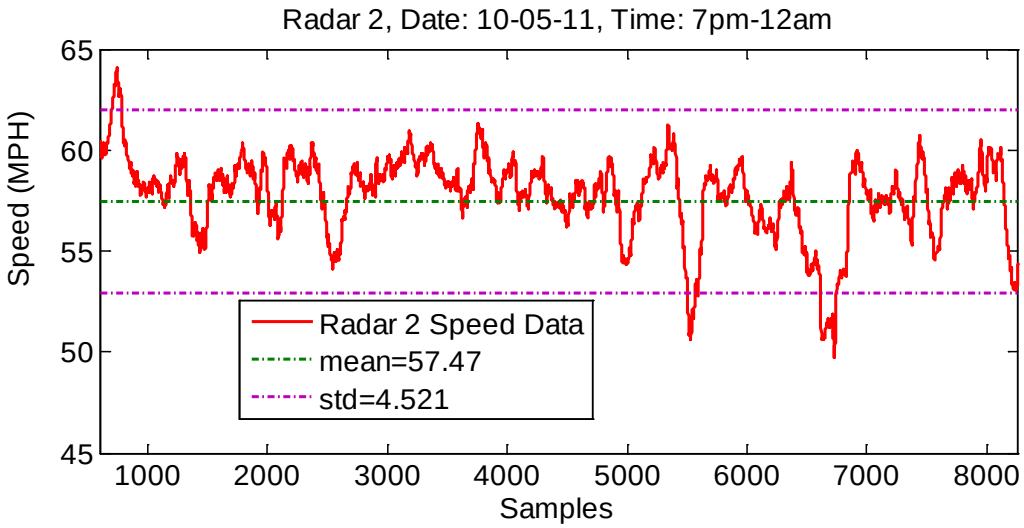

Figure 85: Radar 2: 7PM-12AM.

The new analysis results for October 5 from 18:00 to 23:59, and October 6 from 00:00 to 15:00 are shown in Figures 86 and 87, where each bar represents the average speed for 15 minutes detected by the K-band radar sensors (R1, R2), blue and yellow color are for R1 and R2, respectively.

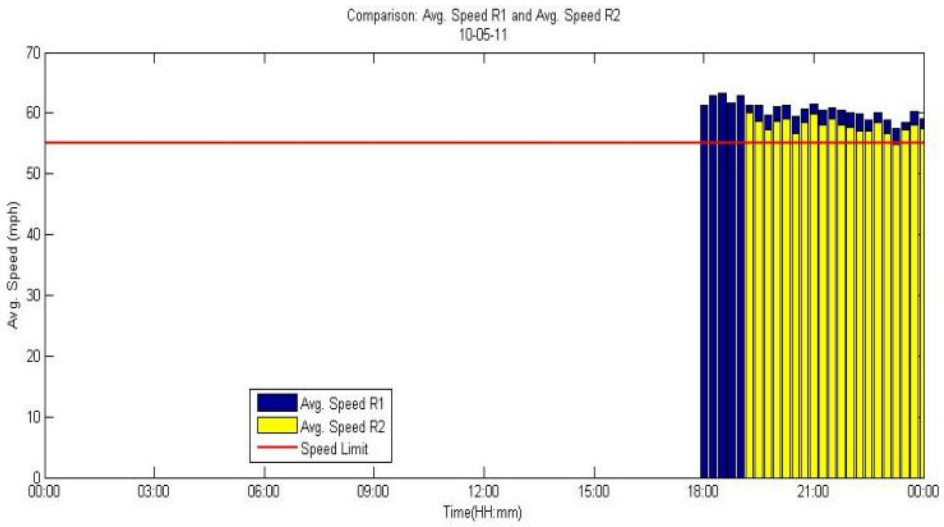

Figure 86: Comparison of the average traffic speed collected by the two K-band radar sensors on 10-05-11 with histograms.

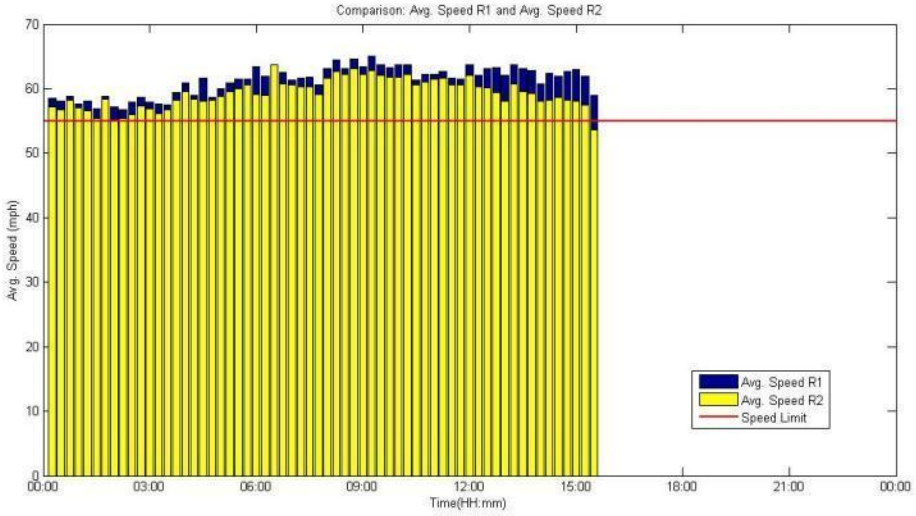

Figure 87: Comparison of the average traffic speed collected by the two K-band radar sensors on 10-06-11 with histograms.

6.6.4 Data Records and Analysis of November 2011

Before the data collection tests in November, the team has worked on improving the system by optimizing the number of bytes in the communication among nodes, having a better seals on the packages, fixing interference issues on the data logger, repairing/replacing the weather-damaged modules, calibrating the sensors, and reducing the power consumption of the system.

Therefore, in the last week of October, a traffic data collecting from 4 consecutive days was performed on the same site (I-40), those new improvements were reflected in the overall system performance in terms of obtaining better synchronization of the nodes (Figures 88 and 89) and reliable speed data.



Figure 88: Warning lights in dim mode at night when no speeding is detected.



Figure 89: Warning lights flashing when speeding is detected.

The test started on Sunday, 30 October, at 15:28 and finished on Thursday, 3 November, at 13:47 (the system was still working very well at the time of finishing data collection). Table 3 shows general information of the field test such as hours of operation, weather conditions, and a deployment diagram of the system. The results for each day are shown in Figures 90-94. In these plots, each bar represents the average speed for 15 minutes detected by the K-band radar sensors (R1, R2), blue and yellow color are for R1 and R2, respectively. From the figures, we can observe speed reduction in smart barrel zone during day/night hours, and the average

speed during nights is in the range of 52 mph to 60 mph, which further shows the effectiveness of the system despite of the limited number of nodes used for this test.

Table 3: Nov 2011 field test general information

Dates	Hours of Operation	Weather Condition
10-30-11	R1-> 15:28 to 23:59 R2-> 16:18 to 23:59	Normal
10-31-11	R1, R2 -> 24 hours	Normal
11-01-11	R1, R2 -> 24 hours	Windy
11-02-11	R1, R2 -> 24 hours	Normal
11-03-11	R1-> 00:00 to 13:47 R2-> 00:00 to 13:52	Windy

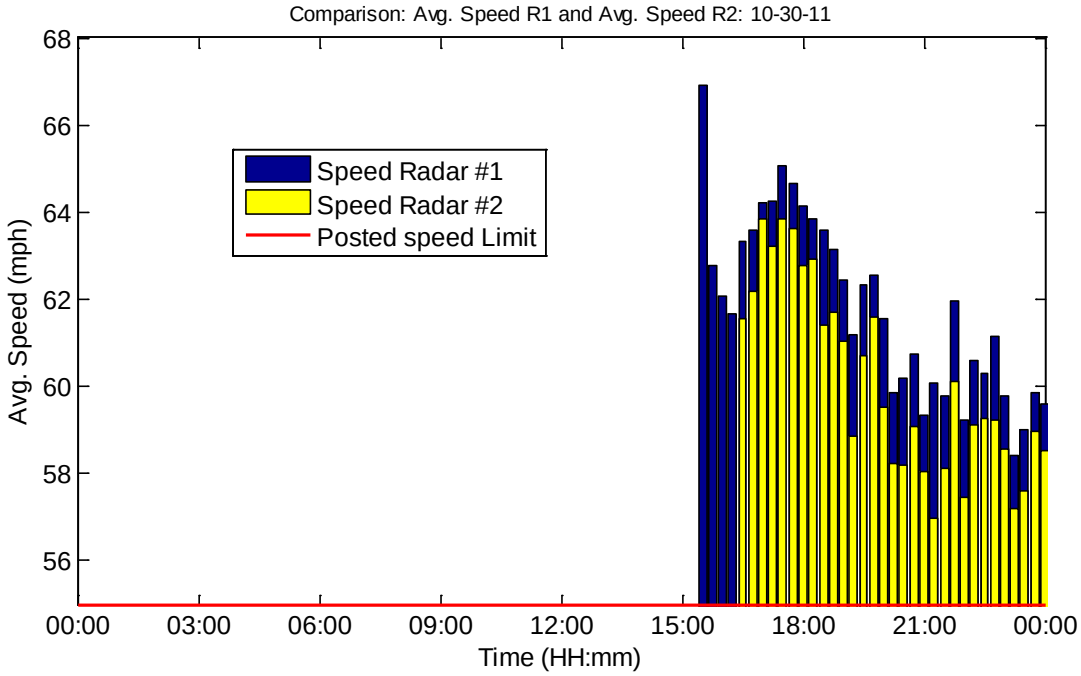

Figure 90: Comparison of the average traffic speed collected by the two K-band radar sensors on 10-30-11. Radar sensor 1 was set up at 15:28, and Radar sensor 2 at 16:28.

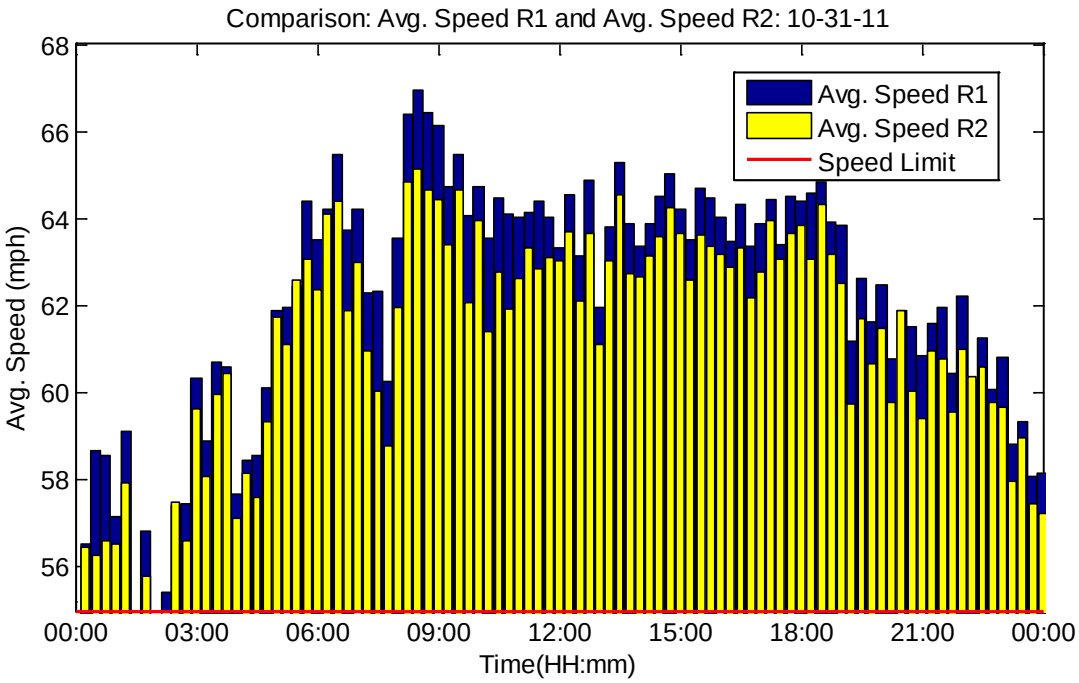

Figure 91: Comparison of the average traffic speed collected by the two K-band radar sensors on 10-31-11.

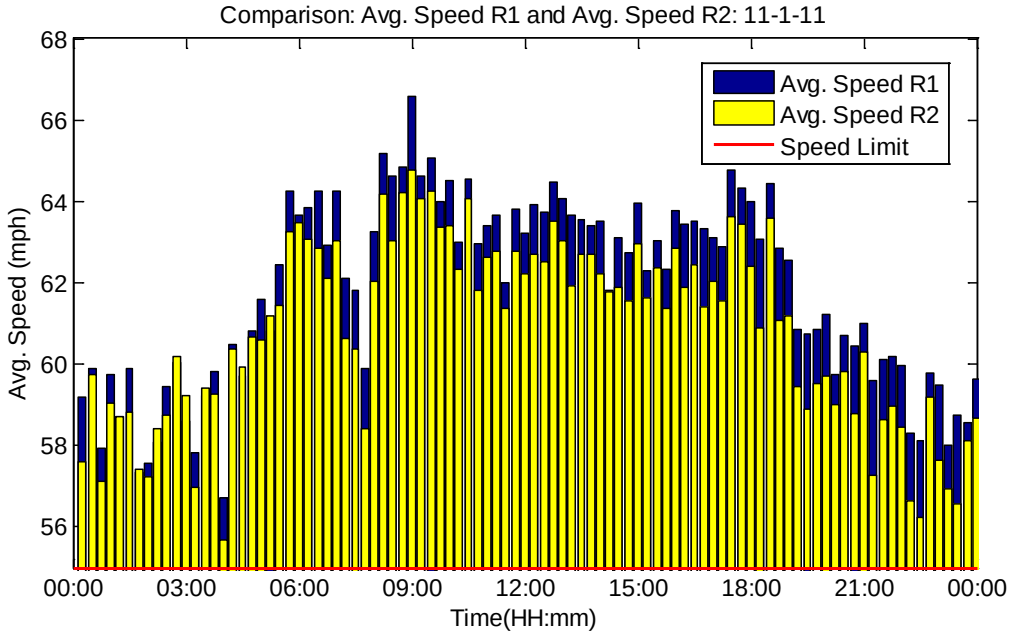

Figure 92: Comparison of the average traffic speed collected by the two K-band radar sensors on 11-01-11.

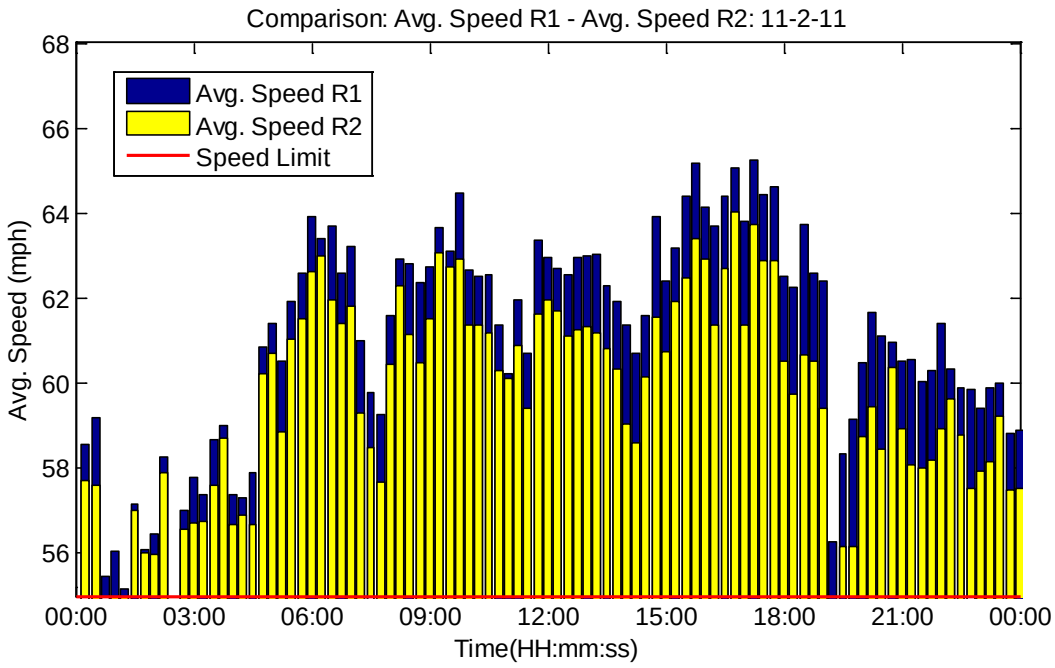

Figure 93: Comparison of the average traffic speed collected by the two K-band radar sensors on 11-02-11.

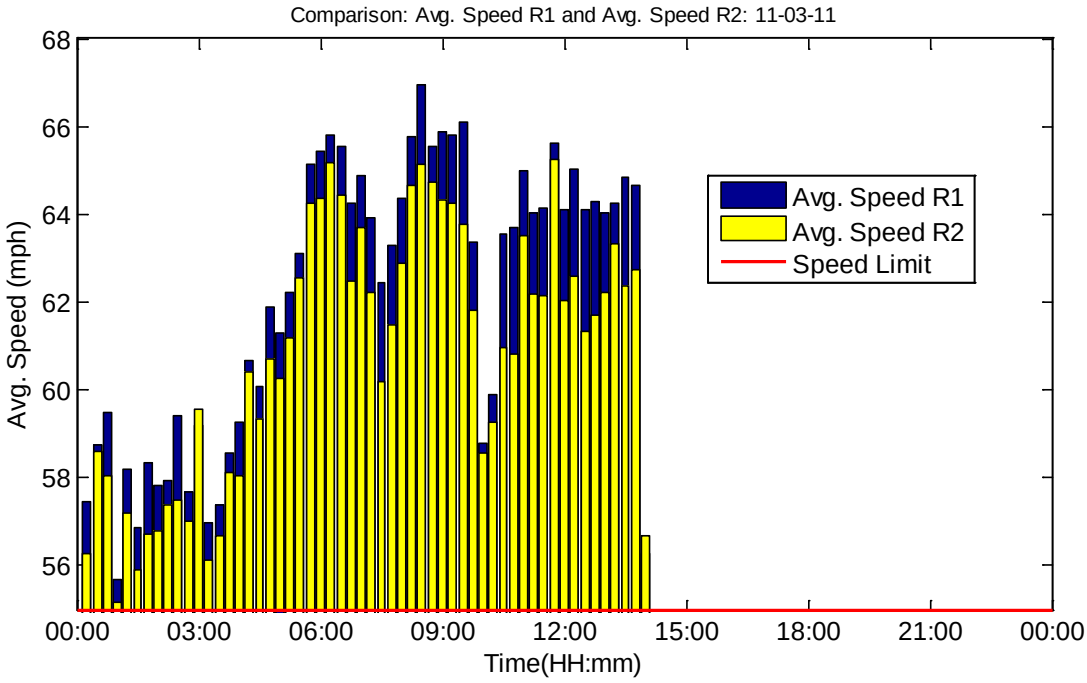

Figure 94: Comparison of the average traffic speed collected by the two K-band radar sensors on 11-03-11.

7. Conclusions and Recommendations

Through this one-year project, the basic concept of ZigBee network based smart barrel system has been demonstrated, through network simulation, system integration, and field deployment. The system integration task has been the highlight of this project, through which we have implemented and optimized a distributed sensing, communication and control software system into the prototype platform. The latest low-power ZigBee radios, millimeter wave radar sensors, as well as high brightness LED control were successfully integrated into a package with the same size of the existing barrel light product. The promising indications of the system effectiveness have been obtained, by comparing the average traffic speed entering and leaving the smart workzone. Further investigations are recommended to better determine the effectiveness of the system, impact on the traffic flow, and quantitative measurements of the safety enhancement. A more compact, lower power smart barrel node design with both speeding and congestion detection capability has already been initiated.

REFERENCES

Sullivan J. M. Winkler C. D., Hagan M. R. (2005), "Smart Barrel for an Adaptive Queue-Warning System", Project report of Transportation Research Institute, The University of Michigan, Ann Arbor, MI.

i-Cone Products Website (2011), http://iconeproducts.com/

Xu Y. and Qi H (2004), Distributed Computing Paradigms for Collaborative Signal and Information Processing in Sensor Networks", Journal of Parallel and Distributed Computing, 64 (8): 945-959.

The ZigBee Alliance (2011), www.zigbee.org.

Atmel Corporation. ATmega328P,ATmega1280 datasheet (2011), http://www.atmel.com/dyn/products/

OPNET Modeler Network (2011), www.opnet.com.

Solar-Masters, Type-B Warning Lights, www.solar-masters.com

Arduino Open-Source Electronics website (2011), www.arduino.cc

Texas Instruments. MAX232 datasheet (2011), www.ti.com/product/max232